

**AD-A280 898**



**CARDIVNSWC-TR-61-94-11** Process Control Development for the Spray Forming Process

**CARDIVNSWC-TR-61-94-11**

**Carderock Division  
Naval Surface Warfare Center**

Bethesda, Md. 20084-5000

(1)

**CARDIVNSWC-TR-61-94-11 June 1994**

**Survivability, Structures, and Materials Directorate  
Technical Report**

**Process Control Development for the  
Spray Forming Process**

by  
**Rochelle D. Payne**

**DTIC  
ELECTE  
JUN 29 1994  
S F D**

**DTIC QUALITY INSPECTED**

**94-19685**



**Approved for public release; distribution is unlimited.**

**94 6 28 0 4 6**

## TABLE OF CONTENTS

ABSTRACT .....	1
ADMINISTRATIVE INFORMATION.....	1
ACKNOWLEDGMENTS .....	1
INTRODUCTION .....	2
SPRAY FORMING PROGRAMS .....	3
SPRAY FORMING .....	4
NEURAL NETWORKS.....	6
Description .....	6
Back-Propagated Neural Networks.....	9
NEURAL NETWORK FEASIBILITY .....	10
Surface Roughness Sensor .....	10
Run Evaluation and Preparation .....	10
Neural Network Development.....	12
Results and Discussion .....	14
NEURAL NETWORK ACCURACY.....	18
Run Preparation and Evaluation .....	19
Neural Network Development.....	20
Neural Network A Results .....	23
Neural Network B Results .....	25
Neural Network C Results .....	27
PROCESS SIMULATOR .....	30
Gas/Metal Ratio Prediction .....	30
Neural Network Predictions.....	31
PART-ON-CALL PROGRAM.....	34
SUMMARY.....	35
CONCLUSIONS AND RECOMMENDATIONS .....	36
APPENDIX .....	38
REFERENCES .....	41
DISTRIBUTION .....	42

Accession For	
NTIS CRA&I	<input checked="" type="checkbox"/>
DTIC TAB	<input type="checkbox"/>
Unannounced	<input type="checkbox"/>
Justification .....	
By .....	
Distribution /	
Availability Codes	
Dist	Avail and / or Special
A-1	

## LIST OF FIGURES

Figure 1. Schematic of the spray forming process. ....	5
Figure 2. Diagram of a biological neuron. ....	7
Figure 3. Diagram of an artificial neuron (processing element). ....	8
Figure 4. Diagram of the arrangement of a typical neural network. ....	8
Figure 5. Diagram of two-dimensional gradient of error curve with local and absolute minimas and maximas. ....	9
Figure 6 Diagram showing longitudinal slice removed from the final tube (A). This lengthwise slice is then sliced diagonally to correspond with time based measurements (B). ....	11
Figure 7. Graph showing the variation of porosity throughout run A. ....	12
Figure 8. Diagram showing the different components of the training vectors used in this study. Each component is further classified as an input or an output. ....	13
Figure 9. Diagram showing the three different neural networks and the five different test files. It should be noted that the neural network trained with all the data was tested with 3 different test files. ....	13
Figure 10. Graph showing the prediction of the neural network and actual porosity values when the neural network is trained with a set of data and then tested with the same set of data. ....	14
Figure 11. Graph showing the neural network porosity prediction and actual porosity values when the neural network is trained with 3/4 of the original data set and tested with the remaining 1/4. ....	15
Figure 12. Graph showing neural network porosity prediction compared to actual values for a neural network trained with four test runs and tested with one run. ....	16
Figure 13. Graph showing the neural network prediction for exhaust gas temperature and RMS surface roughness value for a neural network trained with the entire original data set and tested with a data set in which only time was varied. ....	17
Figure 14. Graph showing the neural network prediction of porosity for a neural network trained with the entire original data set and tested with a data set in which only time was varied. ....	17
Figure 15. Graph showing the variation of porosity with variations in gas/metal ratio and melt temperature. ....	18
Figure 16. Diagram of longitudinal slice removed from the tube (A). This longitudinal slice is then cut perpendicularly (B). ....	20
Figure 17. Graph showing neural network porosity predictions to variations in the gas/metal ratio and the spray height. ....	21
Figure 18. Graph showing neural network yield predictions to variations in gas/metal ratio and spray height. ....	22
Figure 19. Graph showing the neural network A's porosity predictions for run P. ....	24
Figure 20. Graph showing neural network A's porosity predictions for run Q. ....	24
Figure 21. Comparison of neural network A's yield predictions to the actual yields. ....	25
Figure 22. Neural network B's porosity predictions for run P. ....	26
Figure 23. Neural network B's porosity predictions for run Q. ....	26
Figure 24. Graph showing the neural network B's yield predictions compared to the actual yields	

of runs P and Q. ....	27
Figure 25. Comparison of neural network's porosity predictions to actual porosity values for run P. ....	28
Figure 26. Comparison of neural networks porosity predictions for run Q.....	28
Figure 27. Graph showing neural network C's yield prediction compared to actual yield values of runs P and Q. ....	29
Figure 28. Diagram showing user interface for gas/metal ratio predictions from basic process parameter settings. ....	31
Figure 29. Diagram showing the main form of the spray forming process simulator.....	32
Figure 30. Diagram showing the "Change Parameters" function of the process simulator. ....	33
Figure 31. Diagram showing the main form of the process simulator with visible assumptions box. ....	34
Figure 32. Diagram showing the "backwards" process simulator with visible assumptions box. ...	35

### LIST OF TABLES

Table 1. Process Parameters and Part Properties for runs A-E. ....	11
Table 2. Process parameter settings and results for runs F-Q.....	19
Table 3. Process parameter values chosen for hypothetical test file. ....	21
Table 4. Standard and maximum deviations for porosity and yield predictions (neural networks A, B, and C). ....	29

## **ABSTRACT**

**Spray forming is an alternate alloy production technique to both conventional and powder metallurgy methods. In an effort to develop process control of this process, relationships must be established between process parameters and product quality parameters. Because mathematical modeling of the spray forming process has not yet been able to determine well-defined relationships between process parameters and product quality, neural networks were employed to more clearly define this relationship. It was the goal of initial neural network development to prove the feasibility of neural network use in spray forming control. Because this initial work was successful, the focus of subsequent development was on determining and improving the accuracy of these neural network predictions. Not only can neural networks successfully predict trends in quality data, but they are as accurate as an experienced operator in predicting quality outputs. Finally, process control development resulted in a Windows compatible software program that puts neural network predictions within easy access for the spray forming plant operator.**

## **ADMINISTRATIVE INFORMATION**

**This research was conducted by the Physical Metallurgy Branch (Code 612) of the Carderock Division of the Naval Surface Warfare Center (CDNSWC) and was sponsored by the center's Materials Technology Manager, Ivan Caplan (Code 0115). The work was in support of the Intelligent Processing Program and was performed under work units 1-2812-753 (FY 93) and 1-6120-703 (FY 94). The work was performed under the supervision of Dr. Om P. Arora, Head, CDNSWC Code 612.**

## **ACKNOWLEDGMENTS**

**The author wishes to thank Dr. Angela Moran, formerly of CDNSWC (Code 612) and now at the United States Naval Academy, and the following CDNSWC employees: Mr. William Palko, Mr. Richard Rebis, Mr. Allen Matteson, Mr. Craig Madden, Mr. Robert Mattox, Mr. Steven Szpara and Mr. Paul Kelley. Dr. Moran was the group leader of the Spray Forming Technology Group until August 1993 and her guidance and support is appreciated. Mr. Palko is currently the Group Leader of the Spray Forming Technology Group. Mr. Rebis and Mr. Kelley were responsible for the actual runs studied herein and Mr. Robert Mattox and Mr. Steve Szpara provided significant technical support for these runs and the subsequent metallurgical analysis.. Mr. Matteson and Mr. Madden provided many helpful suggestions on neural network development. Mr. Jeff Jensen, a graduate student at Iowa State University, was a summer intern during the summer of 1993 and helped out in innumerable ways. Thanks are also extended to Tim Zappia and Brad Cleveland of MTS Systems who have been involved in spray forming process**

control from the beginning of the intelligent processing effort.

## INTRODUCTION

Spray forming, like other near net shape manufacturing methods, was developed as an alternative to the conventional casting and wrought manufacturing methods. In addition to producing parts in near final shape, spray forming can produce preforms that are nearly fully dense and with a refined microstructure. Realizing the potential cost savings of this alloy production technique, the U.S. Navy has made a significant investment in exploiting and developing innovative materials processing via metal spray forming. As part of this research and development investment, CDNSWC installed a research facility in 1987 to enable manufacture of prototype components for both commercial and military applications. Several research and development programs have been conducted at CDNSWC, and they are described in the Spray Forming Programs Section.

Osprey <sup>TM</sup> spray forming is a single step gas atomization and deposition process. The Spray Forming section provides a brief background on this relatively new alloy production technique. While the basic concepts of spray forming are relatively straight forward, the interactions between gas, metal and substrate are complicated. As a result, the process of finding the optimal process parameters can be an extensive trial and error iteration. In an effort to eliminate the need for this process and to find quicker and easier ways to determine the optimal process parameters, emphasis has been placed on an intelligent processing program. The main goal of this program is to be able to control preform quality in real time.

Before the quality can be controlled in real time, however, there must be an established relationship between the process parameter data and the spray formed part quality data. The process of finding correlations between the process parameters and the quality data is not an easy task. Many groups have devoted significant time and effort towards this correlation in the form of mathematical modeling. At the International Conference on Spray Forming, an entire session was dedicated to modelling of the process. A review of this session is given in reference 1. While this pursuit is both interesting and necessary for future developments, it has not yet been able to provide information to the plant operator that can help him make decisions about the quality of the part and the process parameters that lead to good part quality. As a result of this, emphasis has been placed on empirical modeling using neural networks in the intelligent processing program at CDNSWC. The objective of this report is to present the results of two studies that utilized neural networks to determine product quality and to use these results to develop a process simulator. An outline of this report is given in the following paragraphs.

The Neural Networks section briefly introduces neural networks and the two subsequent sections highlight two different projects in neural network development. Specifically, in the Feasibility section, neural networks were found to correlate process parameters and quality. In the Accuracy section, three different neural networks were developed and the accuracy of their quality predictions was assessed.

Finally, the Process Simulator section will outline the development of a process simulator which is developed in Microsoft Visual Basic using code created from Neural Works 2

Professional Software. This simulator asks the user for input process parameters and predicts the corresponding outputs, allowing the user to see the probable outputs before actually performing a run.

## **SPRAY FORMING PROGRAMS**

Since 1987, the Spray Forming Technology Group at CDNSWC has established a state-of-the-art metal spray forming facility for the study and exploitation of this near net shape manufacturing process. Spray forming is a single step gas atomization/deposition process which yields ferrous and non-ferrous, near final shape, near fully dense preforms. In the Osprey™ spray forming process, molten metal is rapidly atomized to form a fine spray of particles that are deposited onto a collector or mandrel at rates up to 400 pounds per minute. Spray forming has proven to be a viable and cost effective alternative to conventional metalworking technology for the production of material preforms with properties surpassing those of their cast and wrought counterparts. Current programs at CDNSWC are aimed at certification of the spray formed products, optimization of the process, industrialization of the technology, and development of a reactive metal spray forming capability.

The spray forming effort at CDNSWC began when a program was initiated to identify and develop viable near-net-shape manufacturing methods to reduce the high costs of Alloy 625 piping while still maintaining or improving the properties of the final product. The CDNSWC program indicated that near-net-shape manufacturing, specifically Osprey spray forming, is a viable alternative for producing quality Alloy 625 tubular preforms. The Osprey preforms exhibited a fine, equiaxed microstructure and mechanical properties equivalent to the current specification for the extruded product. Because of the success of the CDNSWC research and development efforts, spray formed Alloy 625 has been selected as a candidate for evaluation under the Foreign Comparative Test (FCT) Program sponsored by the Office of the Secretary of Defense. This program will determine if the Osprey process is certifiable as a viable low cost alternative for conventional piping manufacturing of Alloy 625 piping for naval submarine applications. This program is sponsored by Sharon Allen at the FCT Program Office and technical support is provided by Art Smookler at the Naval Sea Systems Command (NAVSEA).

The Intelligent Processing program has also been undertaken to implement real time sensing of preform temperature, deposition rate, and quality (as indicated by surface properties). The objective of the program is to produce asymmetric components with repeatable microstructural quality. This will be accomplished by developing sensor, control, and manipulator technology to monitor the critical process conditions and modifying parameters during the process via a Fuzzy Logic Controller (FLC). The Intelligent Processing program has been sponsored by ONR, ONT, and at CDNSWC by Ivan Caplan.

Results from the intelligent processing program will be combined with other CDNSWC developments in optimization of the spray forming process and integrated into a 4.5 ton melt capacity, pilot plant facility. The objective of this Manufacturing Technology (MANTECH) program is to industrialize the spray forming manufacturing process in the United States to reduce the cost of military components and to enhance the global competitiveness of U.S. industry. The MANTECH plant will be the largest spray forming facility in the world. The plant has been

manufactured and is scheduled to be installed at a U.S. industrial facility in FY94. This program is sponsored by Steve Linder at the MANTECH Program Office and Mike Petz of NAVSEA.

The Spray Forming Technology Group at CDNSWC is currently developing a **Reactive Metal Spray Forming Facility** to extend the benefits of spray forming to reactive metals such as titanium. The facility will be located at the Nike Site and commissioning is scheduled for late FY94. Initial program funding has been provided by Ivan Caplan of CDNSWC and Mike Petz of NAVSEA.

## SPRAY FORMING

The spray forming plant at CDNSWC (figure 1) consists of a spray chamber, a gas atomizer and a collector attached to the end of a manipulator arm. The metal is induction melted to a desired superheat (usually 80 to 100 degrees Celsius above melting temperature) in an alumina crucible above the chamber. The molten metal is bottom poured from the crucible into the nitrogen purged chamber through an alumina nozzle at rates of 20-75 kg/min. Once inside the chamber, the molten metal stream is atomized by nitrogen gas. In addition to breaking up the stream of molten metal into fine particles, the atomizing gas extracts heat from the particles, protects the particles from oxygen pickup and directs the stream of molten metal onto a mild steel substrate that is at room temperature. The metal particles are in different states of solidification depending on their size and eventually impact the surface of the rotating and translating substrate.[2] The motion path of the manipulator dictates the final part shape. Typically, spray forming produces tubular and billet products. However, the CDNSWC facility has an operational five-axis manipulator with the goal of producing more complicated shapes.

Several of the process parameters listed in figure 1 are used to control a spray forming run. Nitrogen gas overpressure in the crucible is used to control the metal flow rate into the chamber and to control melt purity. During a run, the overpressure is increased in order to keep metal flow constant as the melt height decreases. The atomization gas pressure is responsible for the atomization of the molten metal as well as directing the particle stream. By changing the atomizing gas pressure more or less heat is removed from the metal stream. This affects the state of particles as they collide and impact on the surface of the substrate, and therefore the final quality of the preform. Similarly, the spray height, or particle flight distance, affects the amount of heat in the particles on impact with the substrate. The greater the distance particles must travel towards the substrate, the more heat is dissipated from the particles by convection and radiation. The preform yield is also affected by changes in the spray height. Because the area of the spray cone increases as the spray height increases, the preform yield typically goes down with an increase in spray height.

The scanner varies the angle of the spray with respect to the substrate and can be used to change the spray profile. For example, when forming a tubular without the scanner, the angle between the tubular substrate and the spray remains fixed at 90 deg. and the temperature and mass distributions of the spray profile are bell shaped curves. When used in this study, the scanner oscillates the angle between the spray and the substrate from 87 to 93 deg. This causes a "smoothing" of the bell-shaped temperature and mass distribution, usually leading to reduced porosity. Withdraw rate is the velocity along the axis of the tubular (driving the manipulator arm



either forward or backward). Coupled with the metal flow rate, the withdraw rate dictates the overall preform thickness, while the rotation rate controls the individual layer thickness deposited during each pass under the spray.

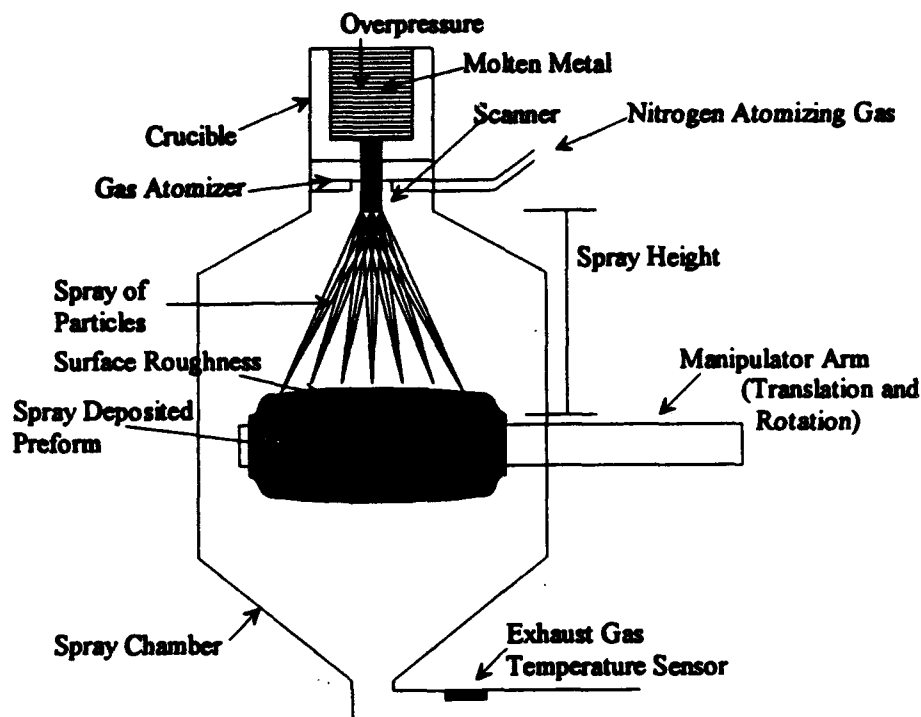


Figure 1. Schematic of the spray forming process.

Several of the parameters described above are combined in a single term called the gas/metal ratio. This single term is a relative measure of heat content of the spray and is a ratio of the gas flow rate to the metal flow rate. The equation used to calculate the melt flow rate is:

$$\text{Metal Flow Rate} = CD \cdot \rho_{\text{metal}} \cdot A_{\text{nozzle}} \cdot \sqrt{2 \cdot \left( G \cdot MH + \frac{OP}{\rho_{\text{metal}}} \right)} \quad \text{Eq. 1}$$

where  $CD$  is the coefficient of discharge (the fraction of the nozzle area effectively used by the metal flow),  $\rho_{\text{metal}}$  is the density of the metal,  $G$  is the acceleration due to gravity,  $MH$  is the height of the metal in the crucible,  $OP$  is the gas overpressure in the crucible and  $A_{\text{nozzle}}$  is the area of the nozzle. During a run, the gas overpressure is increased to offset the decrease in melt height with the goal of keeping the term inside the square root of equation 1 constant. All of the terms in equation 1 are either constant or easily accessible at run time except the melt height and the coefficient of discharge, which must be estimated. The gas/metal ratio is simply the gas flow rate divided by the metal flow rate.

There are several characteristics that can be used to evaluate the quality of a spray formed preform. In this study, yield and porosity are the primary indicators of quality. Previous studies have shown that the porosity of the sprayed preforms reflects changes in process parameters and decreases the amount of usable material, making it a good measure of preform quality.[3,5] The yield is simply the weight of the preform before any subsequent processing divided by the starting

weight of the melt. In order to make optimal preforms, porosity should be minimized and yield should be maximized.

While spray forming offers many advantages over conventional manufacturing methods, the exact relationship between process parameters and quality, as defined by porosity and yield, is hard to define. An experienced operator typically has his own parameter "operating envelope" in which he knows he will get a viable spray formed product. This operator will simply observe a preform as it is being sprayed to determine its relative quality. This operator's decision-making process is based mostly on his experience, memory of past runs and his ability to associate preform appearance with quality. In an effort to copy this experience - based decision making process and to improve on it, the Spray Forming Technology Group at CDNSWC began using neural networks to associate run time process parameters with a preform's porosity and yield.

## NEURAL NETWORKS

### Description

Although a computer can perform mathematical calculations more quickly and accurately than a human being, it still cannot match even a child's capability in recognizing faces, spoken words, and handwriting. In the early days of artificial intelligence, scientists realized the power and versatility of the human brain and how similar computing power could change and improve computers. These scientists decided the best way to mimic the function of the brain was to mimic the form and structure of the brain through software simulations. Human brains are made up of a vast network of interconnected neurons. By constructing a simplified network of interconnected artificial neurons (an artificial neural network), it is possible to mimic a few of the intuitive and indirect human thought processes. This presents great opportunities for many complicated processes that have unclear or weak relationships between inputs and outputs and also provides a mechanism for computers to "learn". To date, neural networks have been successfully used in predicting stock market fluctuations, weather, credit card fraud and even in recognizing handwriting.[6]

Biological neural networks are composed of billions of interconnected neurons ( a single neuron is shown in figure 2). Each neuron acts as a small microprocessing unit and is composed of dendrites (where input from other neurons is received) and an axon (where output to other neurons is sent). There is a small synaptic junction between axons and dendrites of different neurons which provides a way for neurons to communicate with each other. A single neuron will receive a signal from other neurons on its dendrites. If the combined input from these neurons is of sufficient strength, it will cause the neuron to send a signal to other neurons (or "fire"). This is accomplished through the release of chemical neurotransmitters which carry the signal across the synaptic junction from one neuron's axon to another neuron's dendrite. In this way, a signal is transmitted through a group of interconnected neurons.

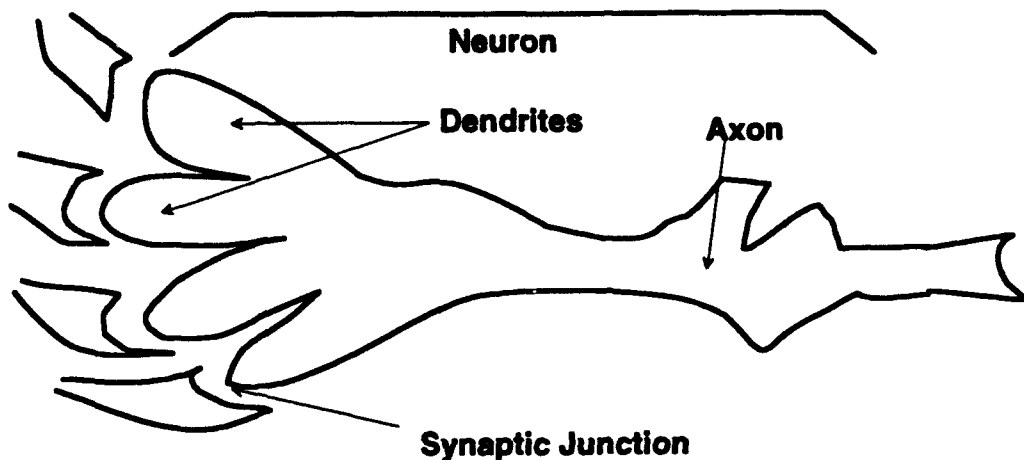


Figure 2. Diagram of a biological neuron.

The modification of connections between neurons is the mechanism that allows human beings to learn. For example, if an event causes two neighboring neurons to fire, the synapse between them will get stronger. The strong connection between two neurons means that if an event causes one of the neurons to fire, the other will fire as well. Often, these connections become reinforced through experience and repetition, perpetuating the learning sequence. A single event may activate many neurons at a time. If a single neuron dies or malfunctions, the network is still able to respond to the event because each neuron has only a small effect on the overall function of the network.[7] The function of the basic biological neuron is relatively simple. The complexities and power of biological neural networks lie in the amount of neurons and the significance of their interconnections.[8]

The artificial counterpart to the biological neuron is the processing element (PE), shown in figure 3. Like the neuron, a PE receives input from many other PE's. These inputs can be summed or combined in a number of ways. In most neural network algorithms, the inputs are summed and the PE "fires" if the combined threshold is above a certain level. Instead of an event triggering a chain of steps, as in traditional computing, events activate many PE's at a time in a neural network. If a single PE were to provide invalid or incorrect sensor data, the network could still function and respond to the event, in a similar way to the biological neural network. In contrast, the malfunction of a single step in conventional computing causes a breakdown of the entire process. Like neurons, the individual functions of PE's are relatively simple. Again, the power of neural network analysis lies in the number of PE's and the level and significance of interconnection.[9]

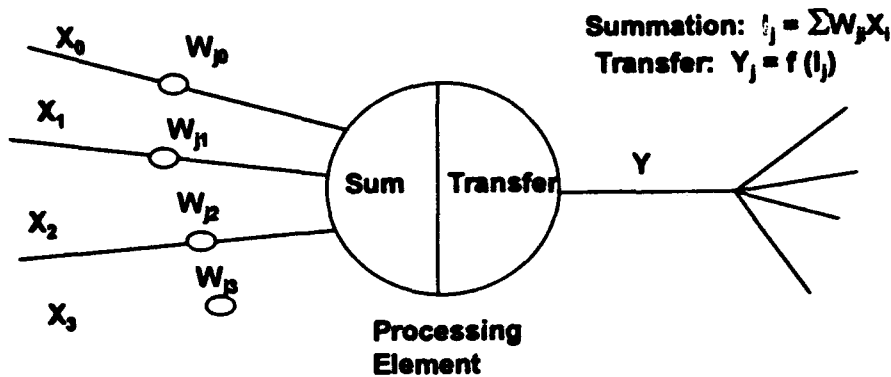


Figure 3. Diagram of an artificial neuron (processing element).

Typically artificial neural networks have an input and output layer and one or more hidden layers. The processing elements in each layer are fully connected to each of the processing elements in the layers before and after it. Figure 4 shows a typical neural network format. The number of PE's in the input layer correspond to the number of inputs for the neural network. Often, the input data is normalized before presentation to the neural network so that no input has undue influence on the network as a result of large values. There can be one or more hidden layers in a neural network. These hidden layers are simply layers of PE's in-between the input and output layers. The number of PE's in each hidden layer and the number of hidden layers is a matter of user preference. Neural network literature, however, recommends only one hidden layer with the number of PE's never to equal the number of patterns in the training set (to guard against memorization).[10] The number of PE's in the output layer correspond to the number of desired outputs from the neural network.

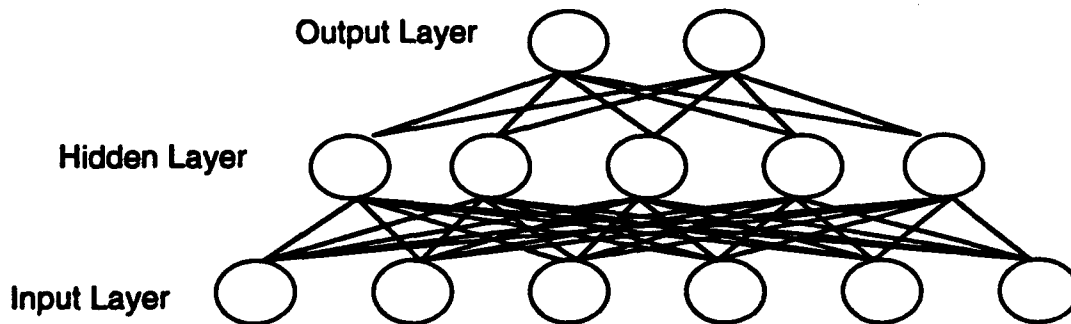


Figure 4. Diagram of the arrangement of a typical neural network.

Like biological neural networks, artificial neural networks are able to learn by strengthening the connections (or weights) between the neurons. An artificial neural network is typically presented with a set of training data, including both the inputs and the corresponding outputs. This set of data will be presented to the neural network several thousand times until a minimum error has been reached. More specific information on neural network training is given in the appendix.

## **Back-Propagated Neural Networks**

The most popular type of neural network is the back-propagated neural network. Its popularity is largely a result of its relative simplicity and ease in training. Neural network development is basically a two step process: training and testing. This section will briefly describe how a back-propagated neural network trains and tests.[10]

In training a back-propagated neural network, several input patterns are presented to the neural network. A particular input pattern causes activity in the first layer which spreads through the hidden layer (or layers) to the output layer. The neural network compares its output values to the actual output values, which will most likely be wrong in the initial stages of training. The algorithm tries to spread "blame" for this error equally among the weights of each of the output PE's and the connections to the layer right before it. Before changes in the weights are implemented, the error back propagates over inter-layer connections all the way back to the input layer. Once the error has propagated back to the input layer, all the weights are modified.[10]

The main goal in back-propagation is to reduce the mean squared error by moving down the gradient of error curve. Ideally, the error curve is a smooth 3-D parabola (or bowl shape). In reality, the error curve is much more complex, and the neural network can easily get stuck at local minima before getting to the lowest possible error. An example of a two-dimensional gradient of error curve is shown in figure 5. Depending on the path chosen by the neural network to reduce error, it could end up at any of the local minima in the gradient of error curve. In order to push the neural network out of the local minima and move on to the absolute minimum, the neural network must be "shook up". There are many tools available to assist in the "shaking up": reinitializing the weights, randomly changing the weights and adding noise to the input data set. Changes can also be made by adjusting the learning rule and the transfer function.[10]

### **Two-Dimensional Gradient of Error Curve**

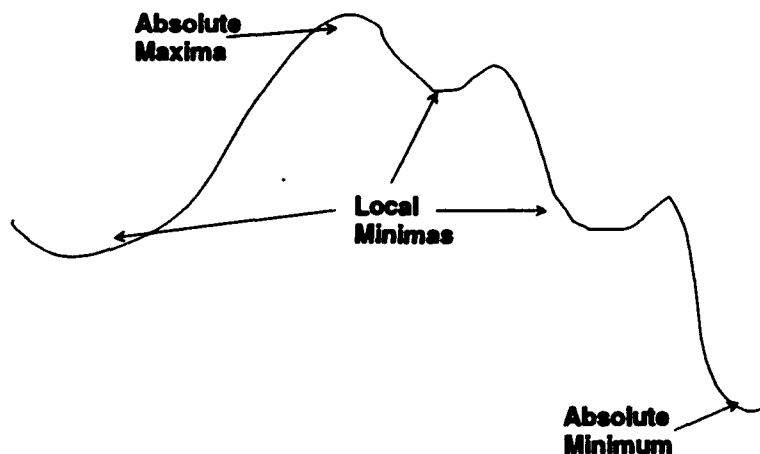


Figure 5. Diagram of two-dimensional gradient of error curve with local and absolute minimas and maximas.

The learning rule used in all neural network development in this paper is the delta rule. For

this learning rule, the network is given an input vector and produces an output vector which is compared to the actual output. If the two values agree, no changes occur. If the values do not agree, weights are modified to reduce the difference. The transfer function used in all neural network development in this paper is the hyperbolic tangent function. The transfer function determines the response of the PE (a function of the input to the PE). Each processing element will pass the hyperbolic tangent of the combination of its inputs. This forces the output of each PE to be from -1 to +1.[11] In the testing phase, the neural network uses the weights modified in learning to predict outputs to a different set of inputs.

## **NEURAL NETWORK FEASIBILITY**

The goal of the intelligent processing program is to find relationships between sensor and process parameter data and quality data. Neural networks were proposed as a way to make this correlation. The following section describes the initial effort to correlate process parameters with end product quality through neural networks. All available data from five previously analyzed Alloy 625 (Nominal amounts of 60% Ni, 20% Cr, 8% Mo, 5% Fe, 4% Nb) tubes was tabulated and used as neural network training data. The ultimate goal of this study was to determine whether neural networks could correlate to process parameters with quality and predict trends in quality expected by experienced operators. The success of this feasibility study determines whether neural networks will be used in future process control developments.

### **Surface Roughness Sensor**

Among the advanced sensing techniques used at CDNSWC to monitor the spray forming process is a surface roughness sensor, described in greater detail in reference 2. The development of the surface roughness sensor was based on the knowledge that an experienced operator will determine the relative quality of a preform by observing the surface characteristics during a spray forming run. The actual sensor consists of an argon laser, a CCD (charge coupled device) camera and roughness determination software. The laser is expanded into a long, thin line and projected onto the preform as it is deposited. The roughness determination software will grab a frame with the laser stripe, digitize it and calculate the root mean square (RMS) value of the roughness in that particular frame. Each frame has a time stamp and can be related back to other time stamped process parameters. Recent sensor work has determined there are correlations between RMS values and porosity values measured after processing [2], as porosity was determined to be the primary indicator of quality.[4] Because surface roughness is used by an experienced operator to determine product quality, it is an appropriate input for the neural network.

### **Run Evaluation and Preparation**

Five spray formed Alloy 625 tubular preforms were used in this study. Each preform was evaluated as-sprayed and was approximately 19 cm long, 10 cm in inner diameter and 2 to 3 cm thick. Properties for the runs are listed in table 1.

**Table 1. Process Parameters and Part Properties for runs A-E.**

Run	A	B	C	D	E
Actual Gas/Metal (kg/kg)	0.65	0.26	0.24	0.33	0.49
Secondary Gas Pressure (Bars)	6.9	6.5	6.2	7.6	6.9
Overpressure Rate (mBars/sec)	0.125	3.46	3.79	3.13	2.17
Nozzle Diameter (mm)	5.28	7.26	7.24	6.81	5.36
Rotational Speed (rpm)	230	230	230	230	230
Withdraw Rate (mm/sec)	2.2	4	4	4	NA
Layer Thickness (mm)	0.10	0.17	0.21	0.18	0.14
Preform Weight (kg)	16.1	15.3	16.0	16.3	15.7
Thickness (mm)	19	25	19	25	19
Run Time (sec)	64	28	24	30	48

The following process parameters were available for these spray forming runs: gas/metal ratio, rotation rate, withdraw rate, spray height and the temperature of the melt, exhaust gas temperature and the surface roughness. All of these process parameters were continuously monitored and recorded during a run at a sample rate of 0.5 Hz. In this section, the artificial neural networks were developed to predict the dependent process variables of exhaust temperature, surface roughness and porosity from the independent process variables of time, melt temperature and gas/metal ratio. The independent variables are those process parameters which can be directly controlled and are believed to have some effect on the quality of the preform. In contrast, dependent variables cannot be directly controlled and are affected by changes in environment.

In order to determine porosity, a 1.25 cm wide longitudinal sample was cut from the wall of each tube (as shown in figure 6a) and then sectioned diagonally (as shown in figure 6b). The sample was sectioned in this way to correlate percent porosity measurements with the sequential points in time when the material was deposited. There were typically five to six sections per run, ranging in thickness from 0.2 cm to 4.0 cm. The porosity in each section was determined using ASTM test B311-58 (Archimedes Method). These porosity values were plotted as a function of time into the run (see figure 7). Porosity values at intermediate times were obtained by interpolating between the measured values. This analysis made it possible to match porosity values to corresponding run time process parameter values which were measured in discrete two-second intervals.

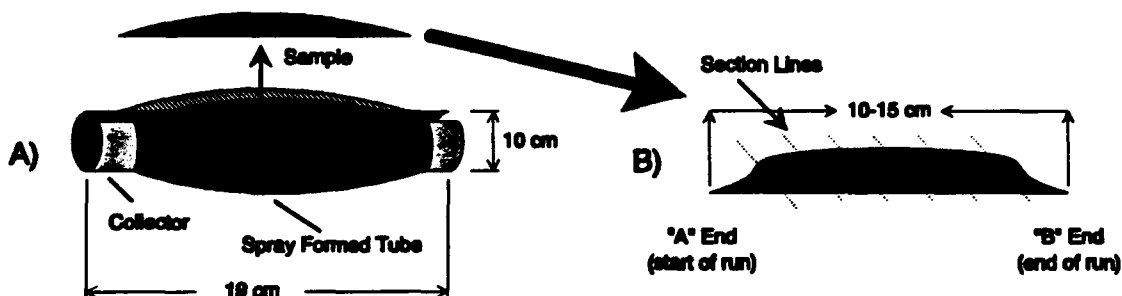


**Figure 6** Diagram showing longitudinal slice removed from the final tube (A). This lengthwise slice is then sliced diagonally to correspond with time based measurements (B).

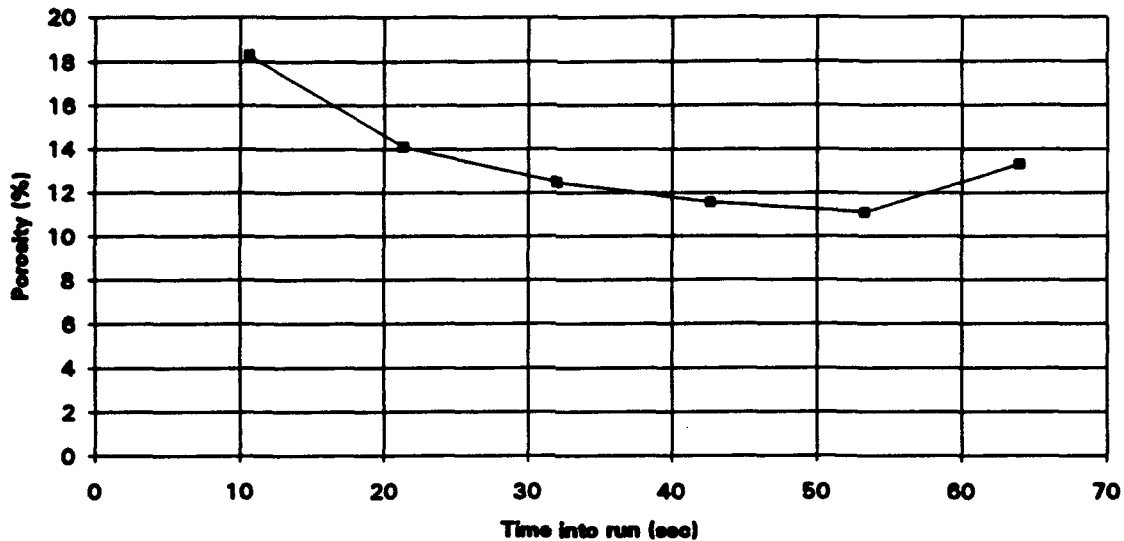


Figure 7. Graph showing the variation of porosity throughout run A.

### Neural Network Development

Three neural networks were developed to prove the feasibility of using neural networks in spray forming, each with a different training data set. All three neural networks were presented with a training set containing time, melt temperature and gas/metal ratio as inputs, and exhaust gas temperature, surface roughness and porosity as outputs. (For the five runs considered, rotation rate, withdraw rate and spray height were invariant and therefore not used as inputs for the neural network.) In addition, it is believed that the quality of the preform at each moment in a spray forming run is dependent on process parameter values several seconds before that moment as well as the process parameter values at that moment. This is particularly apparent in the beginning of the run or the "non-steady state" phase of the run. For this reason, the gas/metal ratio and melt temperature of the three previous time slices are included with the inputs for each moment of time. The five runs together produced 67 training vectors. For the purposes of this particular study, a training vector (shown in figure 8) is defined as a single data point consisting of input values (stimuli) and desired output values (response). The testing vectors are comprised only of the input parameters.



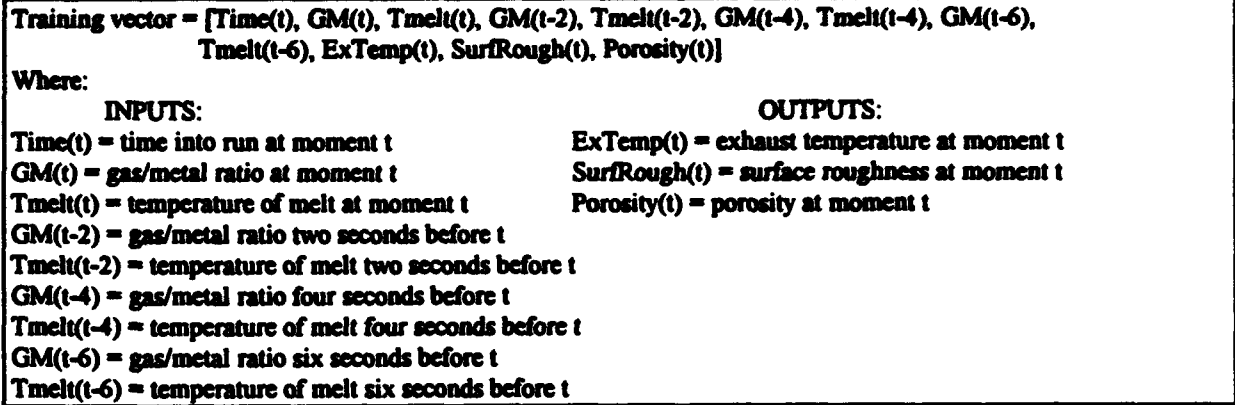


Figure 8. Diagram showing the different components of the training vectors used in this study. Each component is further classified as an input or an output.

Five tests were performed with the three neural networks developed in this paper (see figure 9). The first three tests involve testing the neural network with actual data. The prediction of the neural network is then compared to actual data to assess the performance of the network. The last two tests show hypothetical data to the network. The prediction of the network to hypothetical data is expected to conform with trends based on experience.

Training and Testing Schedule	
Trained with:	Tested with:
all available data	all available data
3/4 available data	1/4 available data
data from 4 runs	data from 5th run
all available data	hypothetical data (time varied)
all available data	hypothetical data (gas/metal ratio, melt temp varied)

Figure 9. Diagram showing the three different neural networks and the five different test files. It should be noted that the neural network trained with all the data was tested with 3 different test files.

The first neural network was trained with all data available then later tested with the same data set. Such a test indicates the existence of contradictory and/or ambiguous training data.

To construct the second and third training sets, specific training vectors were removed from the original data set and the neural networks were trained with these reduced training files. Later, the removed training vectors were presented to the network as test files. In the second training set, 18 vectors were randomly removed which included information from each of the five runs. All of the data associated with run D was removed in the third training set. In both of the neural networks created by these training files, the removed vectors are used later to test the network. The neural network prediction is then compared to the actual value to determine the accuracy of the network. The purpose of these tests is to determine how accurately the neural network can predict information it has not seen.

In an effort to determine the individual effects of the input process parameters, the neural network trained with all the data was tested with two different files of hypothetical input data. The first hypothetical data file held gas/metal ratio and melt temperature constant while varying time. The results of this test indicate whether time has an effect on the process. In the second

hypothetical data file, time was held constant while gas/metal ratio and melt temperature were varied. Specifically, this was accomplished by varying the melt temperature over a range of values. At each melt temperature value, the gas/metal ratio was also varied over a range of values. The resulting three-dimensional plots reveal the effect of gas/metal ratio and melt temperature on the output properties, as well as the optimal operating range for the input parameters.

The neural networks created in this paper were developed using NeuralWorks Professional II software. The configuration for each of the networks consisted of an input layer with nine input PEs (corresponding to the inputs shown in figure 8), two hidden layers of six processing elements each, and an output layer of three processing elements (corresponding to the outputs shown in figure 8).

### **Results and Discussion**

Using the procedure outlined above, three neural networks were created and then tested. The following graphs show each network's prediction of porosity. In the first step, a neural network was created using the entire data set and then tested on the same data set. The graph showing the ability of the network to predict porosity is shown in figure 10. The neural network predicted value agrees with the actual value or is very close to the actual value for most of the data points. This shows that the training file for this neural network contained little, if any, contradictory data. Vectors 1 to 22 are from run A, vectors 23 to 31 are from run B, vectors 32 to 39 are from run C, vectors 40 to 49 are from run D, and vectors 50 to 67 are from run E.

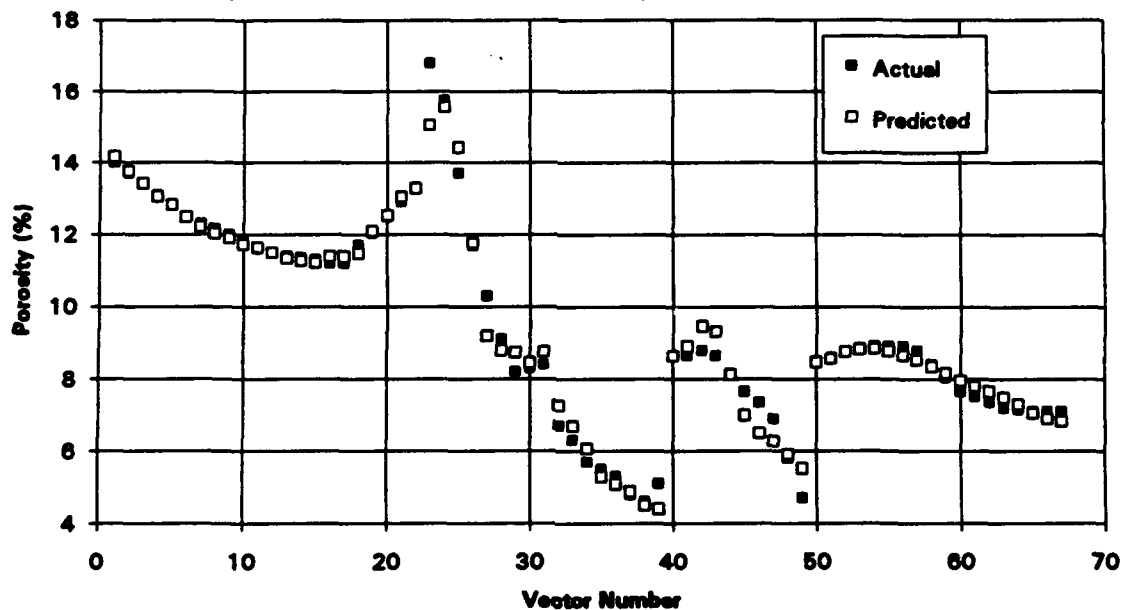


Figure 10. Graph showing the prediction of the neural network and actual porosity values when the neural network is trained with a set of data and then tested with the same set of data.

In the next step of the procedure, approximately 1/4 of the data from the test file was randomly removed before training the neural network. This removed set of data contained

information from each run and was later used to test the neural network. The results of this experiment are shown in figure 11. The neural network's predicted values come very close the actual values, showing that the network can accurately predict data it has not seen before.

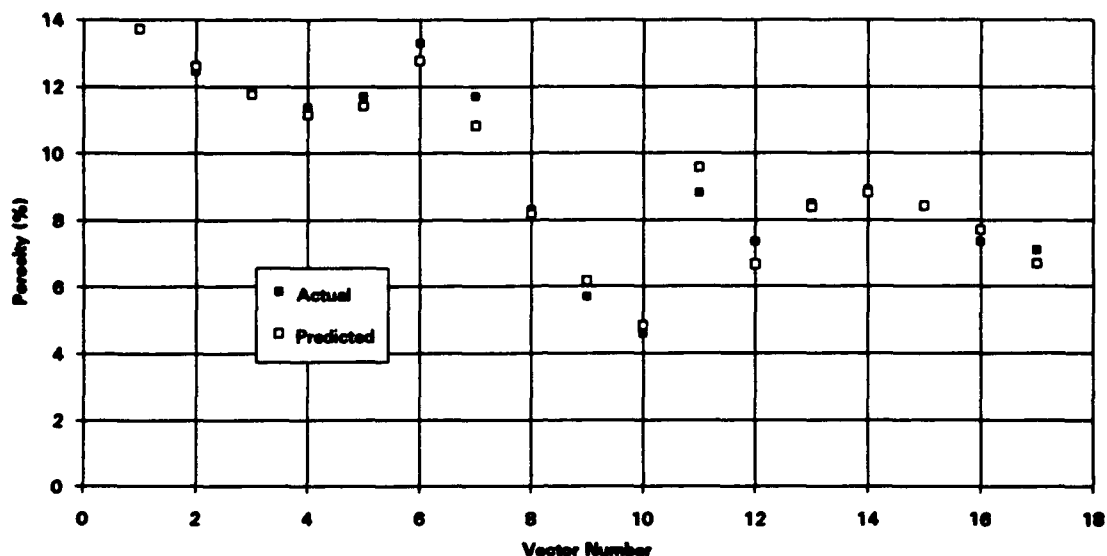


Figure 11. Graph showing the neural network porosity prediction and actual porosity values when the neural network is trained with 3/4 of the original data set and tested with the remaining 1/4.

Again to determine how well the neural network responds to data it has not seen before, a network was trained with four of the five runs and tested with the remaining run. Run D was chosen to be removed for this experiment. The results of the neural network prediction are shown in figure 12. Because each of the five runs is different, each run may contain information not contained in any of the other runs. For this reason, this neural network was not as successful in predicting porosity as the previous network. The neural network predictions are as much as 4% off the actual porosity values, but follow the trends of the actual data. Again, the neural network responded well to data that it has not seen before.

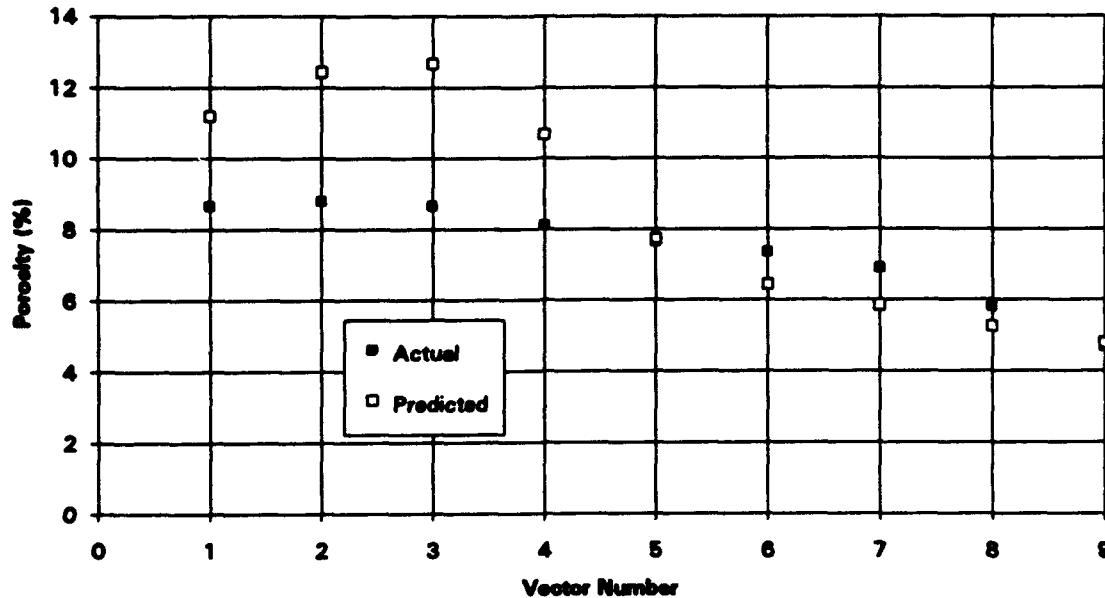


Figure 12. Graph showing neural network porosity prediction compared to actual values for a neural network trained with four test runs and tested with one run.

In the final step of this study, the neural network trained with the entire original data set was tested with two sets of hypothetical data. The purpose of this experiment was to determine the individual effects of the input process parameters on the final part quality. In the first hypothetical data set, the melt temperature and gas/metal ratio were held constant while time was varied from 0 to 60 seconds. The network prediction of exhaust temperature and RMS surface roughness value (1 RMS value = 0.25 mm) for this test file are shown in figure 13. Contrary to what is shown in figure 13, the exhaust temperature starts at room temperature (20 °C) in actual runs. The exhaust temperature starts at about 200 °C in figure 13 because the neural network was not trained with data from the first six seconds of the run (as a result of the temporal nature of the neural network). Thus, the first six seconds for both figures 13 and 14 represent an extrapolation for the network and should be considered accordingly. It should be noted that the exhaust gas temperature seems to level off at about 30 seconds after the run has started, while the RMS value increases linearly starting about 15 seconds into the run. The variation of porosity with time is shown in figure 14. The porosity also levels off, but again not until about 30 seconds after the run has started. It has been a long held belief that the spray forming process does not reach steady state until well into a run. For example, the half first meter (or the "non-steady state" section) of sprayed tube is often discarded in production size plants. The following graphs reinforce this hypothesis.

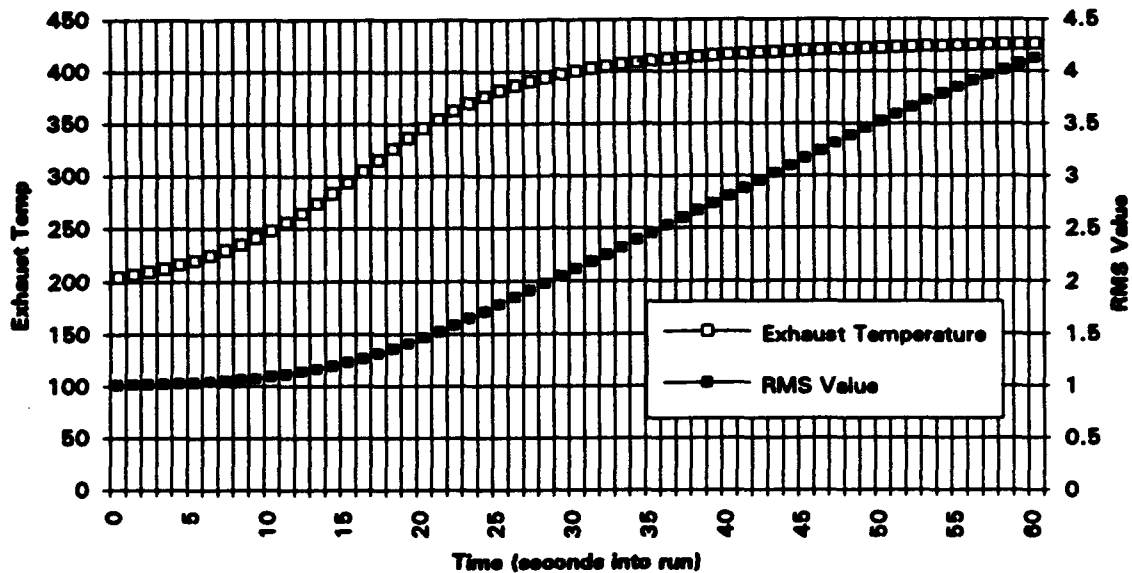


Figure 13. Graph showing the neural network prediction for exhaust gas temperature and RMS surface roughness value for a neural network trained with the entire original data set and tested with a data set in which only time was varied.

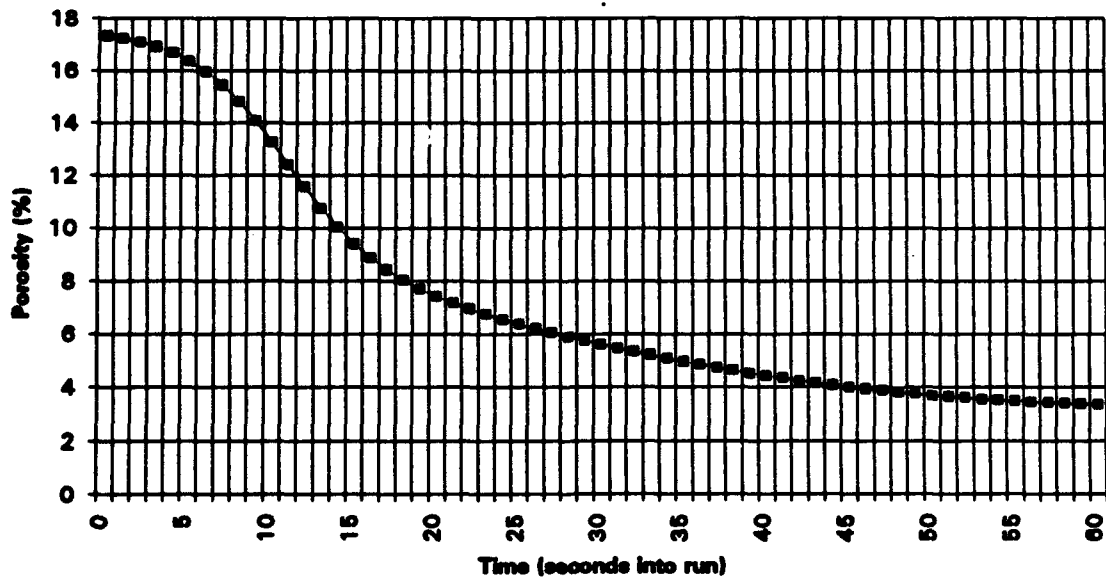


Figure 14. Graph showing the neural network prediction of porosity for a neural network trained with the entire original data set and tested with a data set in which only time was varied.

In the second set of hypothetical data, the melt temperature was varied from solidus (1288 °

C) to the highest recorded melt temperature (1547 °C) in increments of 13°. For each temperature value, gas/metal was varied from the lowest recorded value (0.14 kg/kg) to the highest recorded value (0.66 kg/kg) in increments of 0.03. The neural network prediction for porosity is shown in figure 15. This graph generally follows trends as expected. The highest melt temperature and the lowest gas/metal ratio correlate to the lowest porosity.

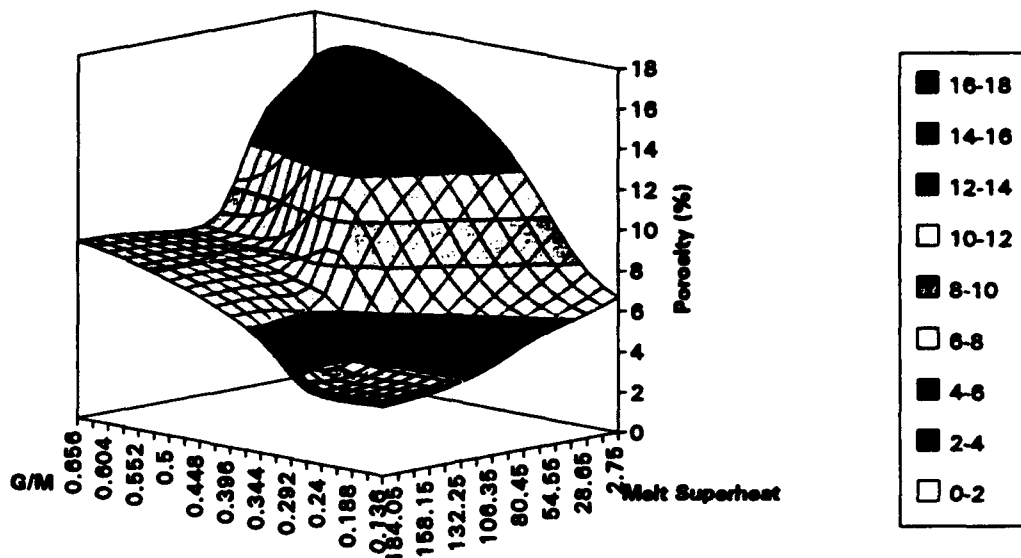


Figure 15. Graph showing the variation of porosity with variations in gas/metal ratio and melt temperature.

Neural networks were able to predict trends in quality values that agree with the predictions of an experienced operator. Because neural networks are successful at predicting trends, the next step in process control development is to use neural networks to predict actual quality values. The neural networks trained in this section were based on a small and limited data file, so no specific process parameter values can be accurately correlated. In order to obtain specific values, a larger and more complete set of runs, made expressly for neural network development, should be used in future neural network development.

### NEURAL NETWORK ACCURACY

Because neural networks were found to successfully correlate process parameters with quality, further neural network development was undertaken to assess the accuracy of neural network predictions. In this section, twelve Alloy 625 tubes were sprayed specifically for neural network analysis. The goal was to spray a broad spectrum of tube qualities using many different process parameter settings, which created a data set appropriate for training the neural network. Some changes were made in the experimental procedure from that described in the previous section. As with the feasibility study, success in this accuracy study will determine whether neural networks will be used in future process control developments.

## **Run Preparation and Evaluation**

Twelve spray formed Alloy 625 (nominal amounts of 60% Ni, 20% Cr, 8% Mo, 5% Fe) tubular preforms were used in this study, all produced at the CDNSWC spray forming facility. Each preform was evaluated as-sprayed and was 25–40 cm long, 19.1 cm in inner diameter and 2.5 to 5 cm in wall thickness. All tubes were produced using the same type of atomizer and a starting charge weight of 97.3 kg. Processing parameters, overall porosities and yields for the runs are listed in table 2. The process parameters for these runs were deliberately varied in order to create a variety in end product quality, shown by the porosity varying from 2.5% to 12.2% and the yields varying from 44% to 78%.

**Table 2. Process parameter settings and results for runs F-Q.**

Run Number	F	G	H	I	J	K	L	M	N	O	P	Q
Nozzle Diameter (mm)	7.14	7.14	7.24	7.49	7.49	7.49	6.73	6.73	7.11	6.73	6.60	6.60
Atomizing Gas Pressure (Bars)	8.0	6.5	8.5	8.8	8.8	8.3	9.3	8.3	10.0	7.9	6.9	5.7
Spray Height (mm)	650	550	550	700	600	650	600	500	550	450	550	600
Rotation Rate (rad/sec)	24.7	18.6	24.8	18.4	18.6	18.6	18.6	18.5	18.8	18.7	18.6	18.5
Withdraw Rate (cm/sec)	0.22	0.42	0.22	0.24	0.24	0.22	0.18	0.32	0.24	0.20	0.22	0.25
Melt Flow Rate (kg/min)	49.1	47.6	48.1	53.9	50.3	47.5	39.9	42.8	43.3	40	38.7	38.7
GMR (kg/kg)	0.52	0.43	0.55	0.51	0.47	0.49	0.70	0.58	0.71	0.63	0.56	0.48
Porosity (%)	5.0	2.5	3.5	6.4	2.7	4.5	12.2	3.8	9.0	3.6	2.9	3.0
Yield (%)	51.1	65.0	57.8	50.0	68.1	56.6	43.8	74.0	45.7	78.1	72.5	70.7

The following process parameters were available for this set of twelve runs: time into the run, gas/metal ratio (as well as gas flow rate and metal flow rate), rotation rate, withdraw (translation) rate, spray height, exhaust gas temperature and whether the scanner was used or not. All of these process parameters were continuously monitored and recorded during each run. In comparison to the previous section, the melt temperature was not available, nor was the surface roughness sensor. In addition to this change, all of the available process parameters were used as inputs for the neural network, while the outputs were simply porosity and yield. The reason for this change in configuration was the determination that all information that is available at run time should be used to help determine outputs. For example, all of the process parameters listed above are available at run time and can be used to give information to the neural network. If the neural network is trained to predict values for these parameters as outputs, it will not serve any useful purpose and the neural network will miss the possible advantage of having this information as an input.

In order to determine porosity, an initial 2.5 cm longitudinal cut was made (figure 16a), and then sectioned perpendicularly to the axis of the tube (see figure 16b). (Please note the difference between figure 16a and figure 6 in the previous section. In figure 6, the slices are diagonal instead of perpendicular.) There were 25 to 40 perpendicular sections per sample, each approximately 1.0 cm in width. The porosity in each section was determined using the procedure described in ASTM

test B311-58. The porosity data was then correlated to time, dividing the duration of the actual run by the length of the preform. The actual porosity values at a particular time were correlated to the process parameter values at the closest matching time. Yield was measured by dividing the preform weight by the initial charge weight.

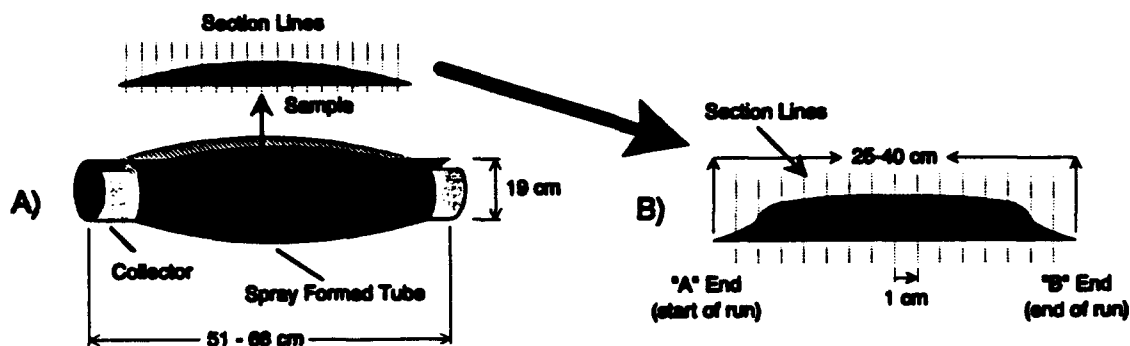


Figure 16. Diagram of longitudinal slice removed from the tube (A). This longitudinal slice is then cut perpendicularly (B).

### Neural Network Development

In previous work [12,13], neural networks successfully associated quality and input process parameters using a relatively small database. The goal in this accuracy section is to further develop neural networks using a larger and more complete database, to evaluate the performance of these neural networks compared to actual runs and to improve their performance if possible. Initially, a procedure similar to those outlined in references 11 and 12 is used. This procedure helps to define an operating envelope for the spray forming process parameters. This information is then used to plan future runs, which are used in testing the neural network to determine the network's accuracy.

Using the procedure outlined in the previous section, a temporal neural network was developed. This neural network was trained with the following data from runs F - O (the first ten of the twelve runs): time into run, gas/metal ratio, spray height, scanner (on or off), withdraw rate, rotation rate and exhaust temperature as well as the same parameters (gas/metal ratio, spray height, scanner, withdraw rate, rotation rate and exhaust temperature) from the previous moment in time. Details on and reasons for the development of this temporal neural network are given in the previous section.

In order to determine the influence of variations in spray height and gas/metal ratio on final part quality (porosity and yield), the temporal neural network was tested with a set of hypothetical data in which gas/metal ratio and spray height were varied systematically while all other process parameters were held constant. The specific values are shown in table 3. The value of time into run was chosen as a result of previous knowledge of the steady state region (as discussed in the previous section), and the other process parameter values were chosen to fall within the range of values in the original training data set.



Table 3. Process parameter values chosen for hypothetical test file.

Process Parameter	Value
Time into run (sec)	50
Exhaust Gas Temperature (deg.C)	420
Gas/Metal Ratio	0.427 - 0.7
Spray Height (mm)	450 - 700
Rotation Rate (rpm)	18.8
Withdraw Rate (cm/sec)	0.225
Scanner	on

The neural network's porosity and yield predictions are shown in figures 17 (porosity) and 18 (yield). Again, details on this procedure are covered in greater detail in reference 12.

In general, figure 17 shows that low porosity values occur at low gas/metal ratios and short spray heights (lower left-hand edge of graph), while high porosity values correspond to high gas/metal ratios and long spray heights (upper right-hand edge of graph). This also agrees with operator experience. The exception to this trend is a pocket of low porosities that extend from gas/metal ratios of 0.43 to 0.57 and spray heights of 525 mm to 625 mm.

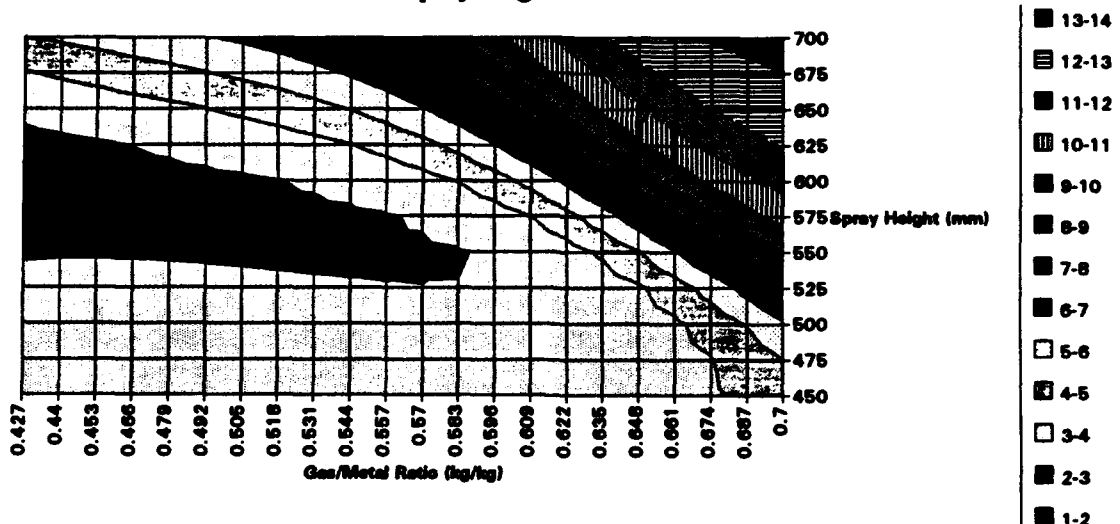


Figure 17. Graph showing neural network porosity predictions to variations in the gas/metal ratio and the spray height.

Figure 18 shows the neural network's yield prediction. Low yield values correspond to high gas/metal ratios and long spray heights, while high yields occur with low gas/metal ratios and short spray heights. This prediction agrees with operator experience and also corroborates with figure 17; the best quality (low porosity and high yield) occurs when spray height is short and gas/metal ratio is low. As noted before, there is one pocket of low porosities shown in figure 17 that does not fall into the general trend. The process parameters for runs P and Q were chosen so that this questionable area could be investigated more fully.

It is interesting to note the gas/metal ratio and spray height which leads to an optimal product (low porosity and high yield). When figures 17 and 18 are juxtaposed, the lowest porosity (2-3%) and the highest yield (75-80%) regions overlap at a small section extending from gas/metal ratio of 0.43 to 0.45 at a spray height of 550 mm.

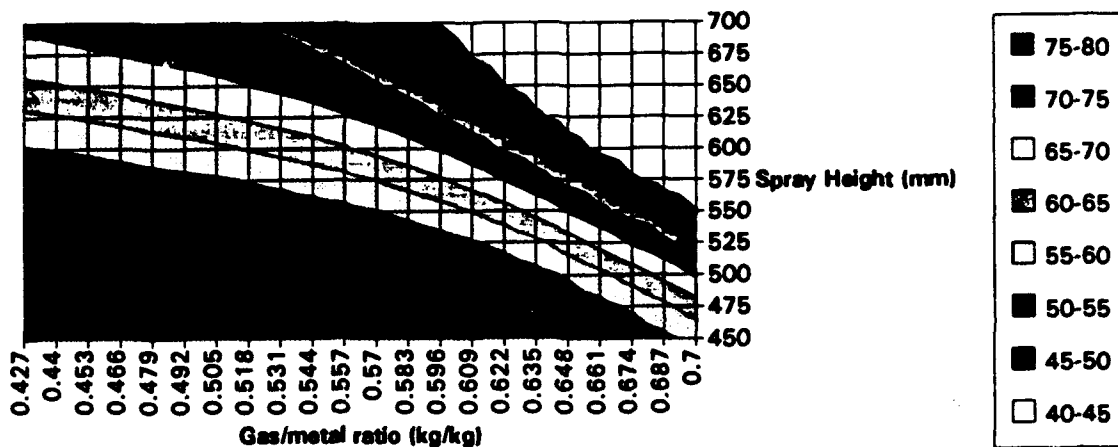


Figure 18. Graph showing neural network yield predictions to variations in gas/metal ratio and spray height.

Figures 17 and 18 show which parameter values lead to the best quality and the neural network's porosity and yield predictions at particular gas/metal ratios and spray heights. While it is accurate to say that a gas/metal ratio of 0.44 and a spray height of 500 mm will lead to low porosity and high yield, it is not necessarily accurate to say that these process parameters will make a preform with 3 to 4 % porosity and 75 to 80% yield because the accuracy of the neural network has not yet been evaluated.

In an effort to evaluate neural network accuracy, runs P and Q are used to test neural networks created with data from the first ten runs. Because it is possible to improve the accuracy of a neural network by improving the quality of information presented to it, three different neural networks are developed using slightly different information. The accuracy of each neural network can be evaluated by comparing the predicted values to the actual values.

Experienced spray forming operators use gas/metal ratio as a relative gage of the amount of heat in the spray formed part. In addition, previous neural network research has shown that gas/metal ratio has a major influence on the preform quality.[12] In this study, three neural networks were each trained with slightly different versions of this important gas/metal ratio. Specifically, the first neural network ("A") was trained with time, gas/metal ratio, spray height, scanner (on or off), withdraw rate, rotation rate and exhaust temperature. In the second neural network ("B"), gas/metal ratio was separated into its two components: gas flow rate and metal flow rate. The reason for the separation was the observation that two runs could have similar gas/metal ratios, but different melt and gas flow rates, leading to different porosities. Because it is a ratio, the gas/metal ratio inherently disguises certain information, which could be essential. In addition, a mass flow rate sensor will soon be implemented on the spray forming plant at CDNSWC, making metal flow rates directly available at run time. In the third neural network ("C"), gas/metal ratio was replaced with secondary gas atomization pressure, gas overpressure and melt nozzle diameter. These three process parameters are used to calculate the gas/metal ratio

along with the melt height and coefficient of discharge (see equation 1). They are used as inputs for the third neural network because their values are directly available at run time, but it should be noted that these inputs do not include all the information necessary to calculate the metal flow rate, and also therefore the gas/metal ratio.

It is the eventual goal of the Spray Forming Technology Group to implement real-time control of the spray forming process, emphasizing the need for simplicity and robustness. For this reason, the temporal orientation of the original neural network will not be used. Only inputs from a specific moment in time will be considered, instead of including the preceding moment of time as was used in the temporal neural network described earlier.

The neural networks in this paper were created using NeuralWorks Professional II software. Each network had from 7 to 9 input PE's and 2 output PE's. Through a series of iterations, 5 PE's were found to be the most effective in the hidden layer. Other settings found to be most effective include the learning rule (delta rule), the transfer function (hyperbolic tangent) and the number of learning cycles (100,000). Again, further details on neural network settings are described in the appendix. The accuracy of the neural network is assessed by calculating the standard deviation of each neural network's prediction from the actual value. The equation used to calculate the standard deviation follows:

$$S = \sqrt{\frac{1}{N} \sum_{x=1}^N (P_x - A_x)^2} \quad \text{Eq. 2}$$

where S is the standard deviation, N is the number of samples,  $P_x$  is the value predicted by the neural network and  $A_x$  is the actual value. The more accurate the neural network, the lower the standard deviation will be. Because the units for porosity and yield are both percentages, the standard deviation is also a percentage. To avoid confusion, however, the percentage unit will be dropped in the following results discussion.

### Neural Network A Results

Neural network A was trained with the following data from runs F - O: time into run, gas/metal ratio, exhaust temperature, spray height, scanner (on or off), withdraw rate, rotation rate, porosity and yield. Figures 19 and 20 show neural network A's porosity predictions for runs P and Q and compare these to the actual values. The standard deviation of the neural network predictions from actual porosity values is 1.7, and the maximum deviation is 4.1. Because the porosity values vary from 0 to 20%, an average variation of 1.7 would be acceptable for research purposes at CDNSWC. For example, most uses of spray formed parts require fully dense material. The neural network can be used to determine the porosity parameters that lead to the lowest possible porosity. Because spray forming rarely produces material completely without porosity, some subsequent processing is usually necessary. If the neural network porosity prediction is off the actual porosity by an average of 1.7, there will be a slight change in the amount of subsequent processing and in the amount of material that is lost because of the subsequent processing.

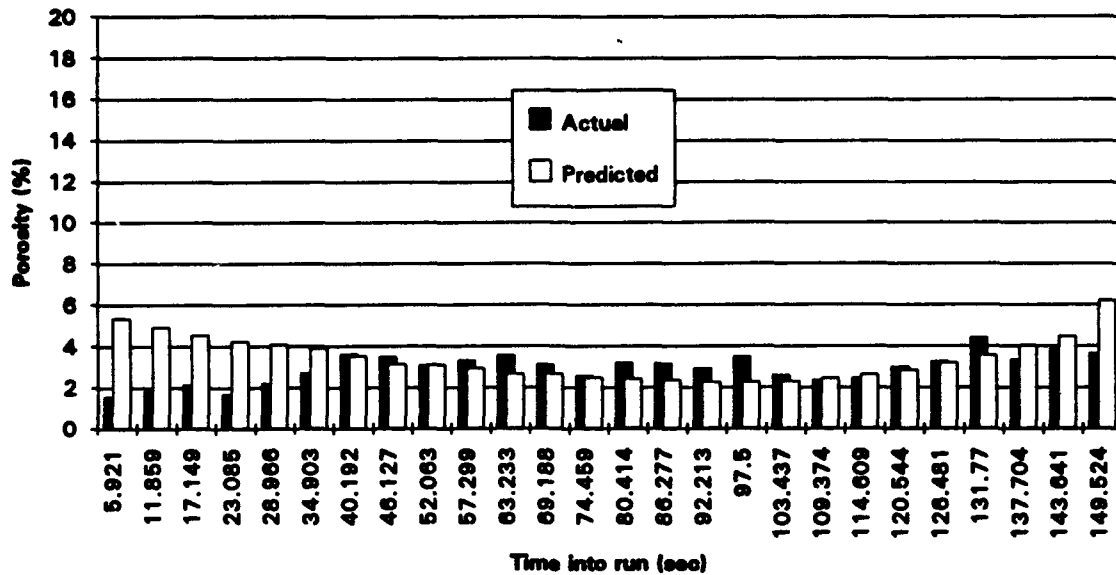


Figure 19. Graph showing the neural network A's porosity predictions for run P.

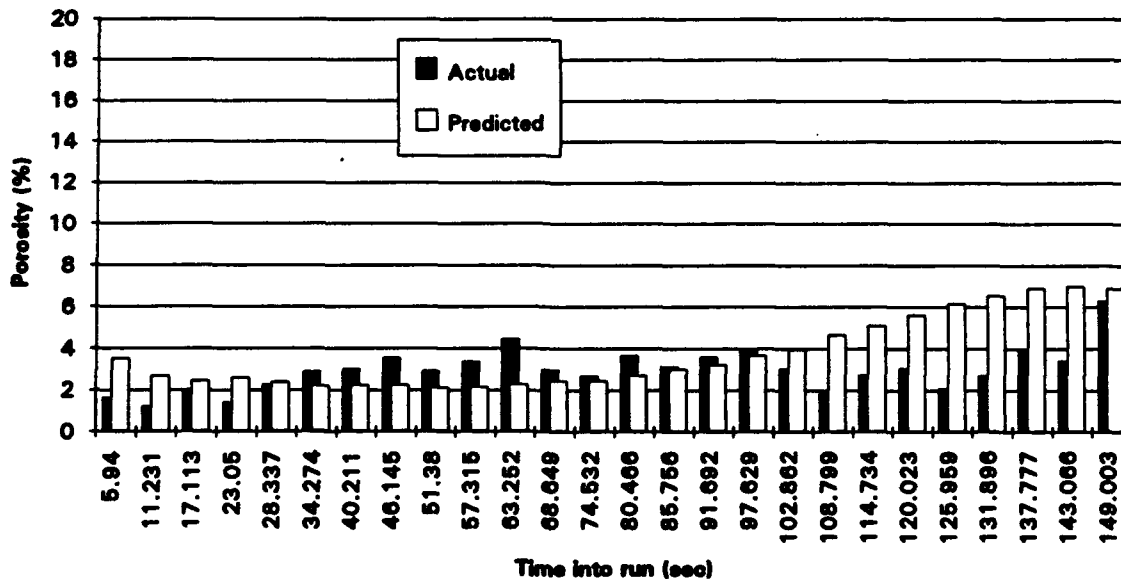


Figure 20. Graph showing neural network A's porosity predictions for run Q.

The yield predictions of neural network A are shown in figure 21 and compared to the actual yields. It should be noted that the yield measured here is a function of the entire run. However, it was necessary to treat yield as a variable with time in constructing the neural network training sets. For this reason, when a neural network is presented with a set of inputs, it predicts both porosity and yield. The porosity values can be analyzed on an individual basis, but the yield

value only has meaning for an entire run. Thus, the values shown in figure 21 represent the average of neural network A's yield predictions for an entire run.

The standard deviation between the neural network's yield predictions and the actual values is 5.6, and the maximum deviation is 13.5. The Spray Forming Technology Group has estimated that an experienced operator's best yield guess is approximately  $\pm 10$ , so neural network A can predict yield with slightly better accuracy than an experienced operator.

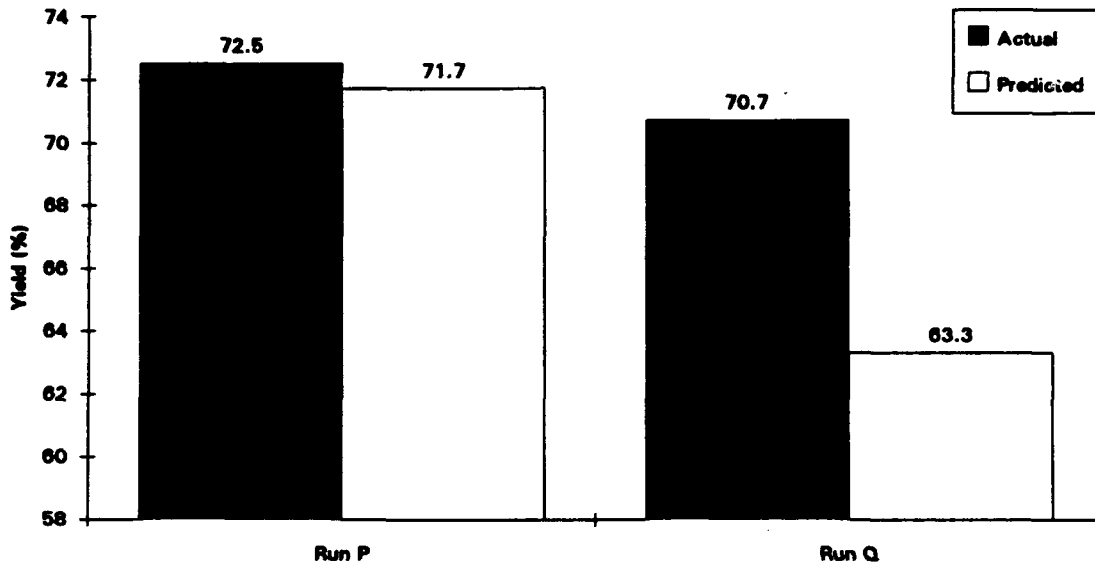


Figure 21. Comparison of neural network A's yield predictions to the actual yields.

### Neural Network B Results

For neural network B, the single input of gas/metal ratio was separated into gas flow rate and metal flow rate and all other inputs were the same as in neural network A. Figures 22 and 23 show neural network B's porosity predictions and compare those to the actual values. The standard deviation between the neural network's porosity prediction and the actual value is 1.2 and the maximum deviation is 2.7. This is a slight improvement in accuracy over neural network A.

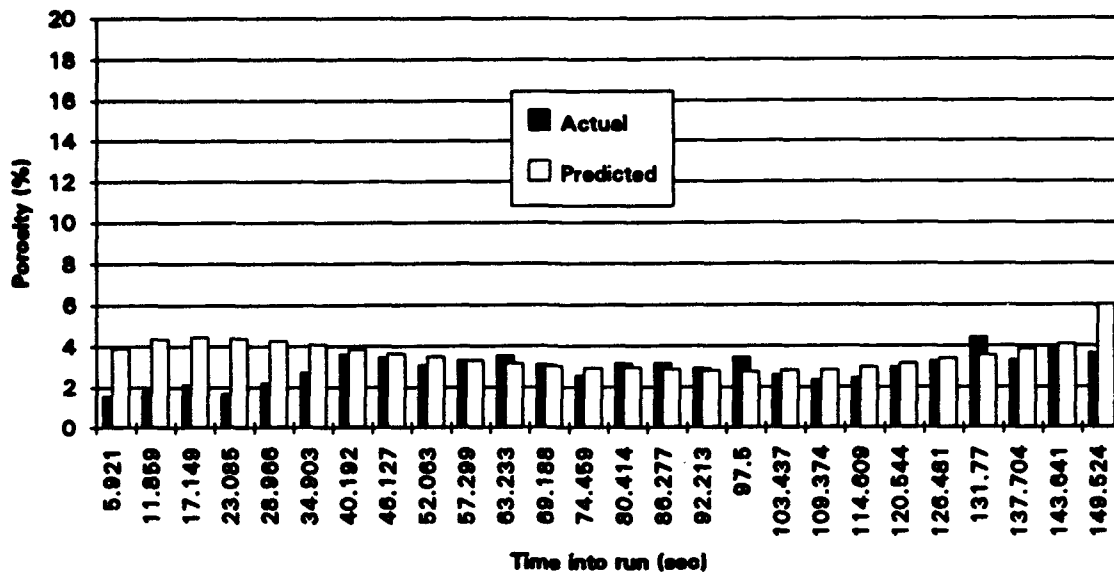


Figure 22. Neural network B's porosity predictions for run P.

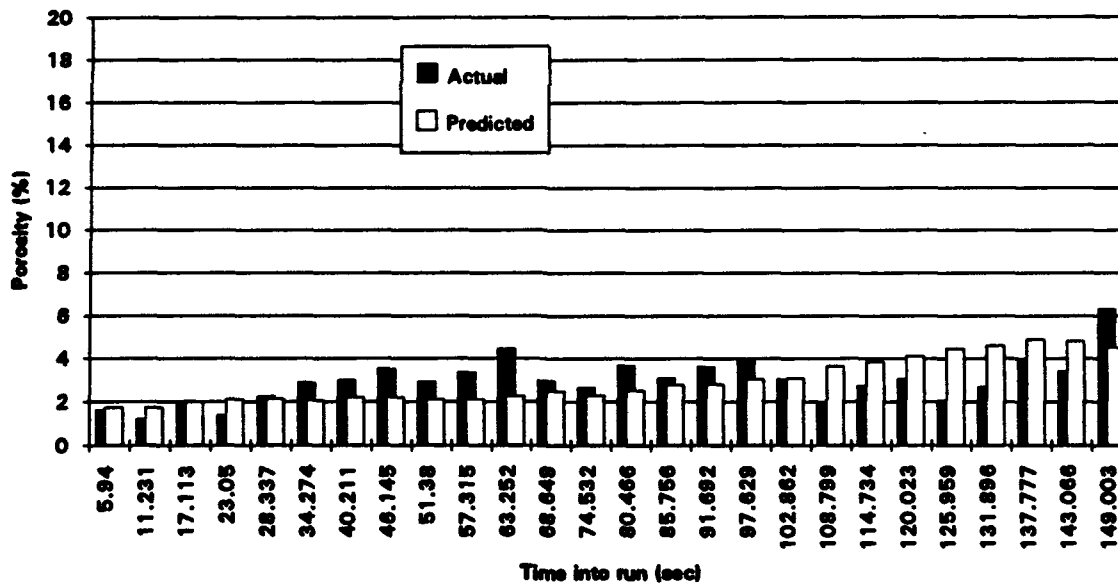


Figure 23. Neural network B's porosity predictions for run Q.

Figure 24 shows the average of neural network B's yield predictions. The standard deviation between the neural network's yield prediction and the actual values is 1.7 and the maximum deviation is 6.3. Again, neural network B shows an improvement in accuracy over neural network A. Because the standard deviation and the maximum deviation are both less than  $\pm 10$  off the actual yields, this network is capable of predicting yield with a lower error than an experienced operator.

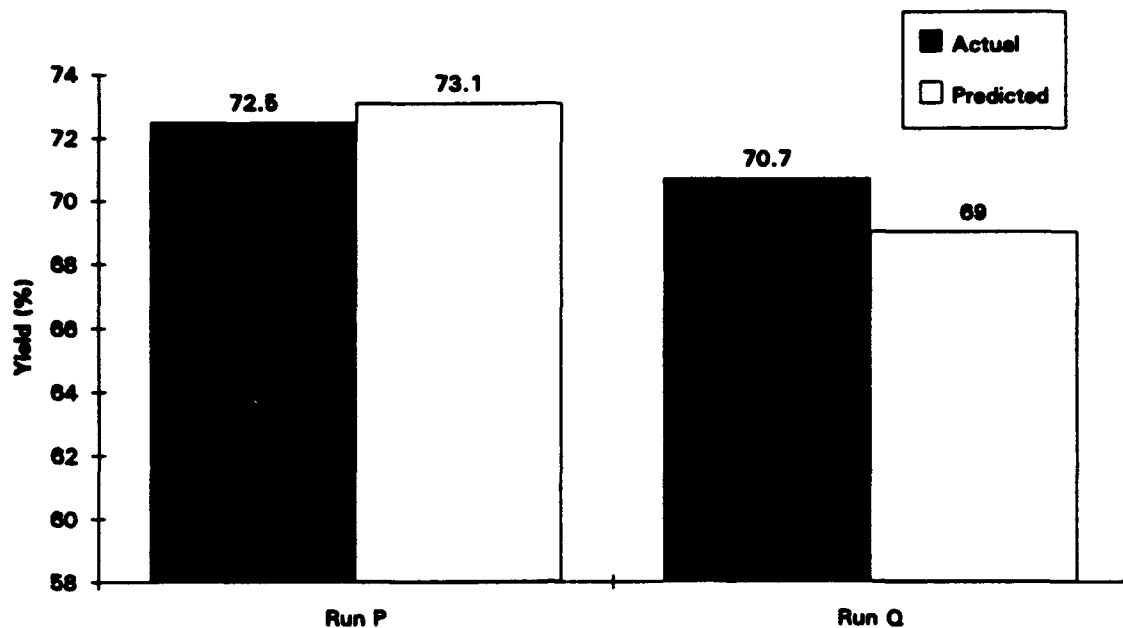


Figure 24. Graph showing the neural network B's yield predictions compared to the actual yields of runs P and Q.

### Neural Network C Results

For neural network C, the single input of gas/metal ratio was replaced with the atomization gas pressure, the gas overpressure and the melt nozzle diameter while all other inputs remained the same as neural network A. Neural network C's porosity predictions are shown in figures 25 (run P) and 26 (run Q). The standard deviation of the neural network's porosity prediction from the actual value is 7.4 and the maximum deviation is 16.0. This represents a significant increase in error over neural networks A and B, and is too high to predict a reliable porosity. For example, the overall porosity of runs G and L are 2.5% and 12.2% respectively. These runs represent the ends of the broad spectrum of Alloy 625 preforms produced in the CDNSWC spray forming plant. This neural network would not be able to tell the difference between these two preforms with a high degree of confidence. For this reason, neural network C would not be useful in predicting porosity.

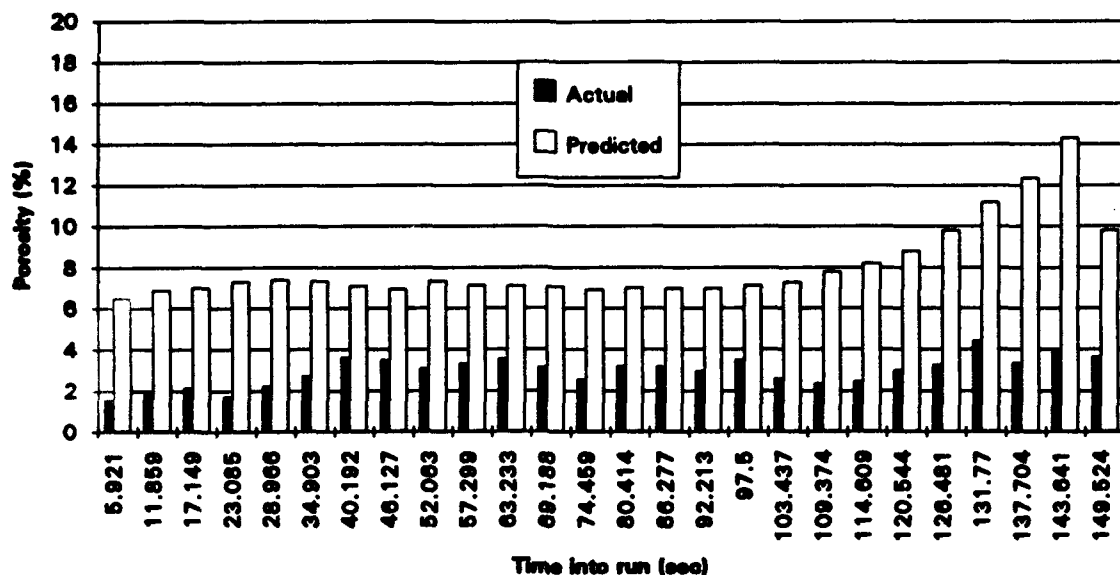


Figure 25. Comparison of neural network's porosity predictions to actual porosity values for run P.

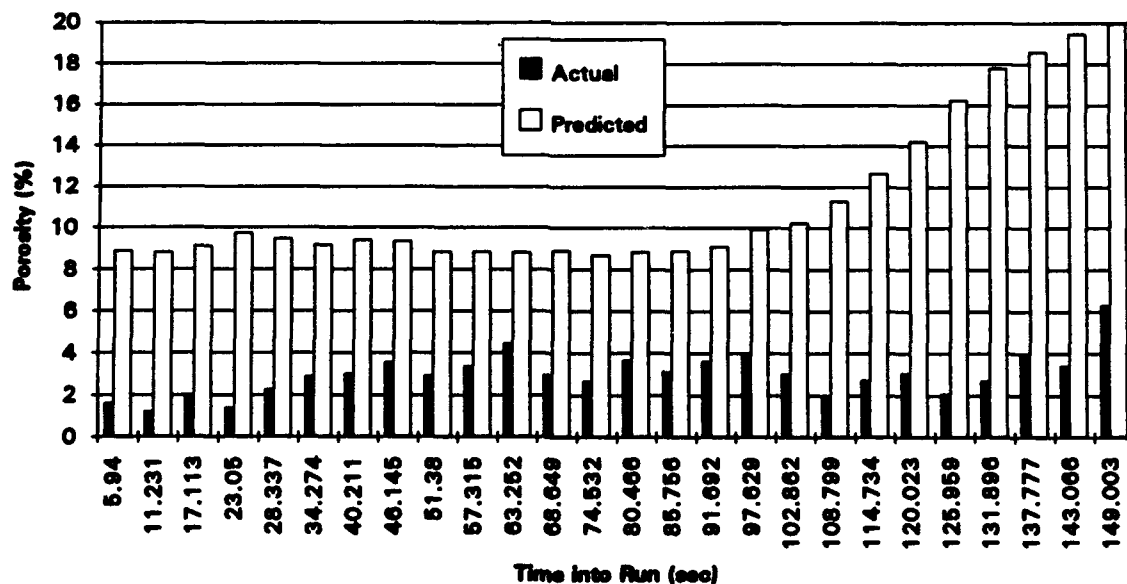


Figure 26. Comparison of neural networks porosity predictions for run Q.

Neural network C's yield predictions are shown in figure 27. The standard deviation of the neural network's yield prediction and the actual values is 11.0 and the maximum deviation is 17.1. Again, this represents a significant decrease in accuracy from neural networks A and B and this neural network would not be as reliable in predicting yield as an experienced operator.



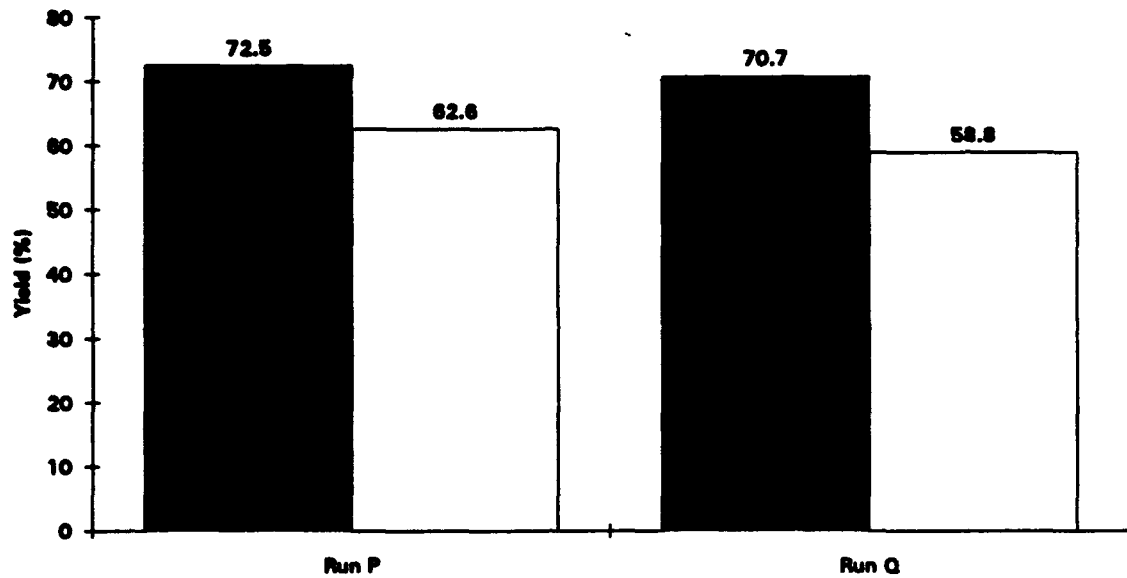


Figure 27. Graph showing neural network C's yield prediction compared to actual yield values of runs P and Q.

Because neural network B was more accurate in predicting yield and porosity than either neural network A or C, the inputs of gas flow and metal flow appear to represent activity in the spray forming chamber most accurately. As stated previously, two runs can have the same gas/metal ratio, but different metal flow rates, gas flow rates and porosities. Separating the gas/metal ratio into gas and metal flow rates improved the neural network accuracy by removing the contradictory information (that the same gas/metal ratio could lead to different porosities). Replacing gas/metal ratio with only the basic parameters that are available at run time (secondary gas pressure, overpressure, nozzle diameter) significantly decreased the accuracy of neural network C. This neural network had the poorest accuracy of the three neural networks, indicating the absence of crucial and unpredictable information, such as melt height. Table 4 shows the standard and maximum deviation values of both yield and porosity for the three neural networks.

Table 4. Standard and maximum deviations for porosity and yield predictions (neural networks A, B, and C).

Neural Network	Standard Deviation - Porosity Predictions	Maximum Deviation - Porosity Predictions	Standard Deviation - Yield Predictions	Maximum Deviation - Yield Predictions
A	1.7	4.1	5.6	13.5
B	1.2	2.7	1.7	6.3
C	7.4	16.0	11.0	17.1

## PROCESS SIMULATOR

Neural networks have proven to be both a feasible and an accurate method for predicting quality parameters in spray forming, as discussed in the two preceding sections. Because both of these studies were successful, the next step in process control development is to actually use neural networks to control and improve the spray forming process. This implementation is a multi-faceted effort. In the long term, the neural networks developed for these studies will be used to generate rules for a fuzzy logic controller. This controller will have a set of rules to determine product quality from different sources, weight the rules according to current conditions, and make changes in the process parameters to improve the quality if necessary. This task is ongoing.

In the short term, the plant operator needs access to the information provided by the neural network in a user-friendly, windows compatible "process simulator". The process simulator should give the plant operator all the process parameter settings necessary in order to proceed with a run as well as a prediction of the quality parameters resulting from the process parameter settings. In using this process simulator, the plant manager can see the probable outputs before actually proceeding with a run and perform a "what if" analysis. This task has been divided into two software applications: "Gas/Metal Ratio Prediction" and "Neural Network Predictions".

### Gas/Metal Ratio Prediction

When planning a run, the plant operator needs to know the approximate pour time, the gas overpressure rate (so that the melt flow rate is constant from the beginning to end of the run), and as a means of comparing one run to another, the melt flow rate and the gas/metal ratio. The calculation of the melt flow rate follows directly from equation 1. At the beginning of the run, all the metal is in the crucible and has a specific melt height which is measured from the top of the metal head to the bottom of the nozzle. The height of the metal can be estimated knowing the melt charge weight, the density of the metal ( $\rho_{\text{metal}}$ ) and the area of the crucible ( $A_{\text{crucible}}$ ) according to the following formula:

$$\text{Melt Height} = \frac{\text{Melt Weight}}{\rho_{\text{metal}} \times A_{\text{crucible}}} + \text{nozzle length} \quad \text{Eq. 3.}$$

The starting melt flow rate is calculated using the melt height and assuming that the gas overpressure is zero. This modifies equation 1 slightly:

$$\text{Metal Flow Rate} = A_{\text{nozzle}} \times CD \times \rho_{\text{metal}} \times \sqrt{2G(\text{Melt Height})} \quad \text{Eq. 4.}$$

With the initial melt flow rate and the melt weight, it is possible to calculate run time using the following equation:

$$\text{Run Time} = \frac{\text{Melt Weight}}{\text{Melt Flow Rate}} \quad \text{Eq. 5.}$$

This equation is valid assuming a constant atmospheric pressure inside the spray forming chamber. It is customary practice to keep the metal flow rate constant throughout a spray forming run. In order to accomplish this task with a bottom poured crucible, the gas overpressure must be increased during the course of a run to compensate for the decrease in metal height. To solve for the overpressure ramp rate, the term underneath the square root symbol in equation 1 must be kept constant throughout a run. Thus, the square rooted term is the same at the start of the run

and at the end of the run:

$$2 \times G \times MH_s + \frac{2 \times OP_s}{\rho_{metal}} = 2 \times G \times MH_e + \frac{2 \times OP_e}{\rho_{metal}} \quad \text{Eq. 6}$$

where the subscript s signifies start of run and the subscript e signifies end of run. By rearranging and dividing by time,

$$OP \text{ Rate} = G \times \frac{MW_s - MW_e}{A_{crucible} \times RT} \quad \text{Eq. 7.}$$

With the melt flow rate and an estimated value for the gas flow rate, it is possible to calculate the gas/metal ratio.

The previous paragraph describes the relatively simple calculations used by spray forming plant operators. These calculations have been combined in a Microsoft Visual Basic Program and the main interface is shown in figure 28. The interface was designed so that the user can make changes in the metal type or one or several of the process parameters and see the resulting changes in the melt flow rate, gas/metal ratio, overpressure rate and run time. Changes in process parameter values are made by simply clicking on the text boxes and changing the values. The interface has also been designed so that the user can input either English unit values or metric and the program will convert the values automatically.

<b>RUN NUMBER:</b>		<input type="button" value="Calculate"/>	
<b>ALLOY:</b> <input type="text" value="alloy 625"/>		<input type="button" value="Close"/>	
<b>Expected CD:</b> <input type="text" value="0.25"/> <input type="radio"/> kg <input type="radio"/> lbs		<input type="button" value="Print"/>	
<b>Melt Charge Weight</b> <input type="text" value="97.3"/> <input type="radio"/> kg <input type="radio"/> lbs	<b>Metal Flow Rate</b> <input type="text" value="0.71"/> <input type="radio"/> kg/sec <input type="radio"/> lbs/min		
<b>Crucible Skull Weight</b> <input type="text" value="2"/> <input type="radio"/> mm <input type="radio"/> in	<b>Gas to Metal Ratio</b> <input type="text" value="0.8"/> kg/kg		
<b>Area Factor of Atomizer</b> <input type="text" value="4"/>	<b>Overpressure Rate</b> <input type="text" value="1.74"/> mBars/sec		
<b>Melt Nozzle Diameter</b> <input type="text" value="6.751"/> <input type="radio"/> mm <input type="radio"/> in	<b>Run Time</b> <input type="text" value="135"/> sec		
<b>Atomization Gas Pressure</b> <input type="text" value="6.27"/> <input type="radio"/> Bars <input type="radio"/> psi			

Figure 28. Diagram showing user interface for gas/metal ratio predictions from basic process parameter settings.

### Neural Network Predictions

The combination of neural network predictions with the calculations described above would give the plant operator a more complete picture of what is likely to happen during a spray forming run. In the Neural Network Accuracy section, the neural network with gas and melt flow as inputs was chosen for further development because of its relatively high accuracy. This neural network

has the following inputs: time into run, exhaust gas temperature, melt flow rate, gas flow rate, withdraw rate, rotation rate, spray height and scanner (on or off). As stated before, the nozzle diameter, the atomizer type, the coefficient of discharge, the melt charge weight and process parameter settings such as the atomization gas pressure and the overpressure rate change the gas and melt flow rates. Thus, the neural network prediction software should have a way for the user to input these basic settings and have the program calculate the resulting gas and melt flow rates to be used as inputs for the neural network. There should also be a display which calculates the gas/metal flow rate as this term is used as a comparison.

Following the guidelines outlined above, a process simulator was developed in Microsoft Visual Basic. The main user interface is shown in figure 29. The user can change any of the parameters listed on the left side of this form by either changing the actual values in the text boxes or by clicking on the horizontal scroll bars underneath the text boxes. The only exception to this is the scanner which is either on or off. Whenever melt flow rate and gas flow rate are changed, a new gas/metal ratio is automatically calculated. When the user is satisfied with all the input values, he can click on the calculate button in the upper right hand side of the form. This function initiates a sequence of calculations which first normalizes the input data, then puts the data through the weights and connections developed by the neural network software. Finally, the output values are denormalized and displayed on the form. After the calculation has been made, the user is free to make changes in any of the input process parameters. When changes are made in any of the input process parameters, the porosity and yield values will appear with a strike-through line. This is to remind the user to click on the calculate button after every change in the input process parameters. Clicking on the print button prints the main form as is.

**Parameters**

**Neural Network Inputs:**

Time into run (sec):

Exhaust Temp (deg. C):

Metal Flow Rate (kg/sec):

Gas Flow Rate (kg/sec):

Spray Height (mm):

Scanner:  On  Off

Rotation Rate (rad/sec):

Withdraw Rate (cm/sec):

Gas/Metal Ratio:

**Neural Network Predictions:**

Porosity (%):

Yield (%):

Buttons: Calculate, Print, Close

Figure 29. Diagram showing the main form of the spray forming process simulator.

As stated earlier, the gas and metal flow rate are the result of calculations based on the

values of atomization gas pressure, melt nozzle diameter, overpressure rate, melt weight and CD. The user can change these basic parameters by selecting "Parameters" in the menu bar and then selecting "Change Parameters". This function will open a dialog box (shown in figure 30) showing the parameters of CD, melt weight and melt nozzle diameter. The user can make adjustments in these parameters in the same way as in the main form: change the value in the text box or in the horizontal scroll bar. When the user is satisfied with the process parameter values, he can click on the Calculate New Flows button which will update the gas and metal flow rate in the main form. Clicking on the close button will take the user directly back to the main form.

**Warning: Changing These Variables May Take the Neural Network Out of its Range of Accurate Predictions. This Decreases the Confidence of the Neural Network Prediction.**

Charge Weight (kg):

CD:

Nozzle Diameter (mm):

Atomizer Type:

Atomization Pressure (bar):

**Calculate New Flows**

**Close**

Figure 30. Diagram showing the "Change Parameters" function of the process simulator.

This dialog box shown in figure 30 appears with a warning. Although it is convenient for the user of the process simulator to change the charge weight, CD and atomizer type, the neural network was trained with specific values for these parameters. By changing these parameter values, the user may take the neural network out of its range of accurate predictions. The neural network will still be able to make a guess, but it should be noted that this guess is made with reduced confidence. In a similar way, the neural network was trained with data from only Alloy 625 runs. Using the process simulator as it is now to make predictions for other alloys will also reduce confidence in the neural network prediction. Further neural network development is necessary in order to improve the confidence for different process parameter values and for different alloys.

Often, it is helpful to print the assumed basic process parameters along with the rest of the data in the main form. By selecting "Parameters" from the menu bar in the main form and then selecting "Show Parameters", these assumed values become visible in the lower right hand corner of the main form (see figure 31). In addition, any changes in the parameters made through the "Change Parameters" function will appear in the "Assumptions" box.

Neural Network Inputs:	
Time into run (sec):	<input type="text" value="60"/>
Exhaust Temp (deg. C):	<input type="text" value="450"/>
Metal Flow Rate (kg/sec):	<input type="text" value="0.7"/>
Gas Flow Rate (kg/sec):	<input type="text" value="0.3"/>
Spray Height (mm):	<input type="text" value="650"/>
Scanner:	<input checked="" type="radio"/> On <input type="radio"/> Off
Rotation Rate (rad/sec):	<input type="text" value="18.8"/>
Withdraw Rate (cm/sec):	<input type="text" value="0.226"/>

Neural Network Predictions:	
Porosity (%):	<input type="text" value="1.89"/>
Yield (%):	<input type="text" value="77.09"/>

Assumptions:	
Nozzle Diameter (mm):	<input type="text" value="7.233"/>
Atomizer Type:	<input type="text" value="4"/>
Charge Weight (kg):	<input type="text" value="97.3"/>
Atomization Pressure (Bar):	<input type="text" value="5.516"/>
CD:	<input type="text" value="0.86"/>

Gas/Metal Ratio:

Figure 31. Diagram showing the main form of the process simulator with visible assumptions box.

The weights and connections used in this software application were taken directly from Neural Works 2 Professional Software, the software program which developed and trained the neural network. When a neural network has been created and tested, the user can select "Flash Code" from the run menu. This flash code function generates "C" code for the neural network and can be pulled directly into Visual Basic. Although a few alterations are necessary the transfer is relatively simple. The calculations involving the basic parameters use the same equations covered at the beginning of this section.

### PART-ON-CALL PROGRAM

The Part-On-Call Program, which is sponsored by CDNSWC's Materials Block, was undertaken in FY94 by the Spray Forming Technology Group. The goal of this program is to use the advantages of the spray forming process and advancements in the Intelligent Processing and MANTECH programs to develop a rapid prototyping process. Ideally, it should take one week from the time a part has been designed and its dimensions entered onto a CAD system to the final machining process.

Given an alloy and a CAD drawing of a axisymmetrical tubular geometry, the Part-On-Call process would generate an appropriate spray process plan, motion plan, preform geometry and preform mandrel design. From these plans, inexpensive and readily removable mandrels would be manufactured and the part would be sprayed. After spray forming, the mandrel would be removed and final NC machining of the part would take place. This approach will allow conical shapes

with varying inside and outside diameters to be produced. Initial target products include non-welded pipe, flange components, tapered tubes and double diameter tubes. The benefit of this approach is a quick turn-around time, and products with superior properties to cast materials.

The process simulator described earlier will be modified in order to generate the spray process plan. This has taken the form of a "backwards" neural network. For example, the user will identify the desired outputs (maximum yield and minimum porosity) and the process simulator will predict the corresponding spray height and gas/metal ratio. Figure 32 shows this user interface. Eventually, this user interface will not only inform the operator what the metal flow, gas flow and spray height should be, but also create an output file - the spray process plan. This spray process plan gives instructions to the program logic control to set certain process parameter values.

**Neural Network Inputs:**

Alloy:

Porosity (%):

Yield (%):

Scanner:  On  Off

Rotation Rate (rad/sec):

Withdraw Rate (cm/sec):

Inside Diameter (mm):

Outside Diameter (mm):

**Neural Network Predictions:**

Metal Flow Rate (kg/sec):

Gas/Metal Ratio:

Gas Flow Rate (kg/sec):

Spray Height (mm):

**Assumptions:**

Nozzle Diameter (mm):

Charge Weight (kg):

Atomizer Type:

Atomization Pressure (Bar):

CD:

**Buttons:** Calculate, Print, Close

Figure 32. Diagram showing the "backwards" process simulator with visible assumptions box.

## SUMMARY

In an effort to develop process control of the spray forming process, relationships must be established between process parameters and product quality parameters. Mathematical modeling of the spray forming process has not yet been able to determine well-defined relationships between process parameters and product quality, so in this study, neural networks were employed to more clearly define this relationship. The objective of this report is to present the results of two studies that utilized neural networks to determine product quality and to use these results in the development of a process simulator.

Initially, the goal was to determine the feasibility of neural network use in spray forming control. Process parameter data and product quality data (porosity) from five spray formed Alloy

625 tubular experiments (50 lb. melt size each) was compiled and used to test and train a neural network. Various test sequences were performed on neural networks to evaluate their effectiveness in spray forming operating conditions. The neural network predictions were then compared to an experienced operator's predictions. The neural network predictions followed the trends as expected by an experienced operator, proving that neural networks are a useful tool in determining product quality.

Because this initial work was successful, the focus of subsequent development was on determining and improving the accuracy of these neural network predictions. A set of 12 Alloy 625 tubular experiments were performed specifically for neural network development. Process parameter data and product quality data (porosity and product yield) from these 12 runs was compiled and used to train a neural network. Three different neural networks were trained using slightly different forms of the same information. One neural network was trained with the separate inputs of gas and metal flow rate and its predicted quality outputs approached the actual quality values within reasonable error. It is estimated that this neural network is actually slightly more accurate than an experienced operator in predicting yield. This particular neural network is used in the process simulator development and will continue to be used in other process control development.

A Process Simulator was developed in Microsoft Visual Basic using code created from Neural Works 2 Professional Software. This simulator asks the user for input process parameters and predicts the corresponding outputs, allowing the user to see the probable outputs before actually performing a run, thereby reducing the number of trial and error runs. This Windows compatible software program puts neural network predictions within easy access for the spray forming plant operator. The process simulator work is continuing using "backwards" neural network. This effort will support the Part-On-Call Program.

## **CONCLUSIONS AND RECOMMENDATIONS**

The development of spray forming process control involves many aspects. Ultimately, spray forming process control should provide real-time computer-based control. The path to this ultimate goal was broken down into several smaller goals, all outlined in this report. The following lists the conclusions and recommendations of this study:

1. In the feasibility section, neural networks were trained on data from five spray formed Alloy 625 tubes and found to predict trends in quality measurements as expected by experienced operators. Neural networks are, therefore, a useful tool in determining product quality in spray formed material.
2. When a larger and more complete database was used to train a neural network in the accuracy section, the neural network predictions were found to be as accurate as an experienced operator in predicting both porosity and yield. So, in addition to being a useful tool, neural networks are also reasonably accurate when trained with appropriate information. This information is advantageous for the inexperienced operator or an experienced operator that is determining the run process parameters outside his region of expertise.
3. Future neural network development should continue with neural network B developed in the accuracy section. A few possible areas of future activity include determining



what other process parameters, besides gas/metal ratio and spray height, have the greatest effect on part yield and porosity, extending this neural network to predict more quality outputs (such as mechanical properties directly) and making quality predictions for other alloys or other geometries.

4. Because neural networks have proven to be an effective means to predict quality outputs based on process parameter inputs, the next step was to provide the spray forming plant operator with easy access to these predictions. By using windows compatible software, the information learned from neural network development is easily accessible to the plant operator. This aids in the planning of runs and allows the operator to perform "what if" analyses.

5. A process simulator using a "backward" neural network is now being developed for the Part-On-Call Program to predict melt and gas flow rates and spray heights. This process simulator will also write an output file which becomes the spray process plan.

## **APPENDIX**

### **STEP-BY-STEP OUTLINE**

The following outline briefly covers each step in the creation of neural networks:

#### **Step 1**

In EXCEL, calculate critical information not contained in the RDF file (i.e. Gas/Metal ratio, gas flow, metal flow, withdraw rate, rotation rate). This information should be kept in a data file and hand compiled with the porosity and yield information (and any other information desired) for each particular run.

EXCEL Macros to help with this step: GMRPRED.XLM.

#### **Step 2**

In EXCEL, create text files (with extension \*.NNA) for training neural network. This training file contains data from actual runs (taken from data file created in step 1), with each of input and output parameters from all the runs contained in a single column.

EXCEL Macros to help with this step: NNSETUP2.XLM

#### **Step 3**

In Neural Works 2 Professional Software, train a neural network using the training set created in step 2.

This step creates a trained neural network and must be saved before exiting NW2 (the file extension given to the trained neural network is \*.NND).

#### **Step 4**

In EXCEL, create text files (with file extension \*.NNA) for testing the neural network trained in step 3. The input columns of this test file must be in the same format as the training set, but may or may not include output columns. In this step, actual data (to test accuracy) or hypothetical data (to test individual effects of process parameters) may be used.

EXCEL Macros to help with this step: NNSETUP2.XLM

#### **Step 5**

In NW2, open the network trained in step 3, and use the recall function to present the test file to the neural network. NW2 will output a \*.NNR file, containing the neural network's predictions.

### **Step 6**

In EXCEL, chart the resulting data and assess the ability of the neural network to predict the outputs.

EXCEL Macros to help with this step: NNSETUP2.XLM.

### **Step 7**

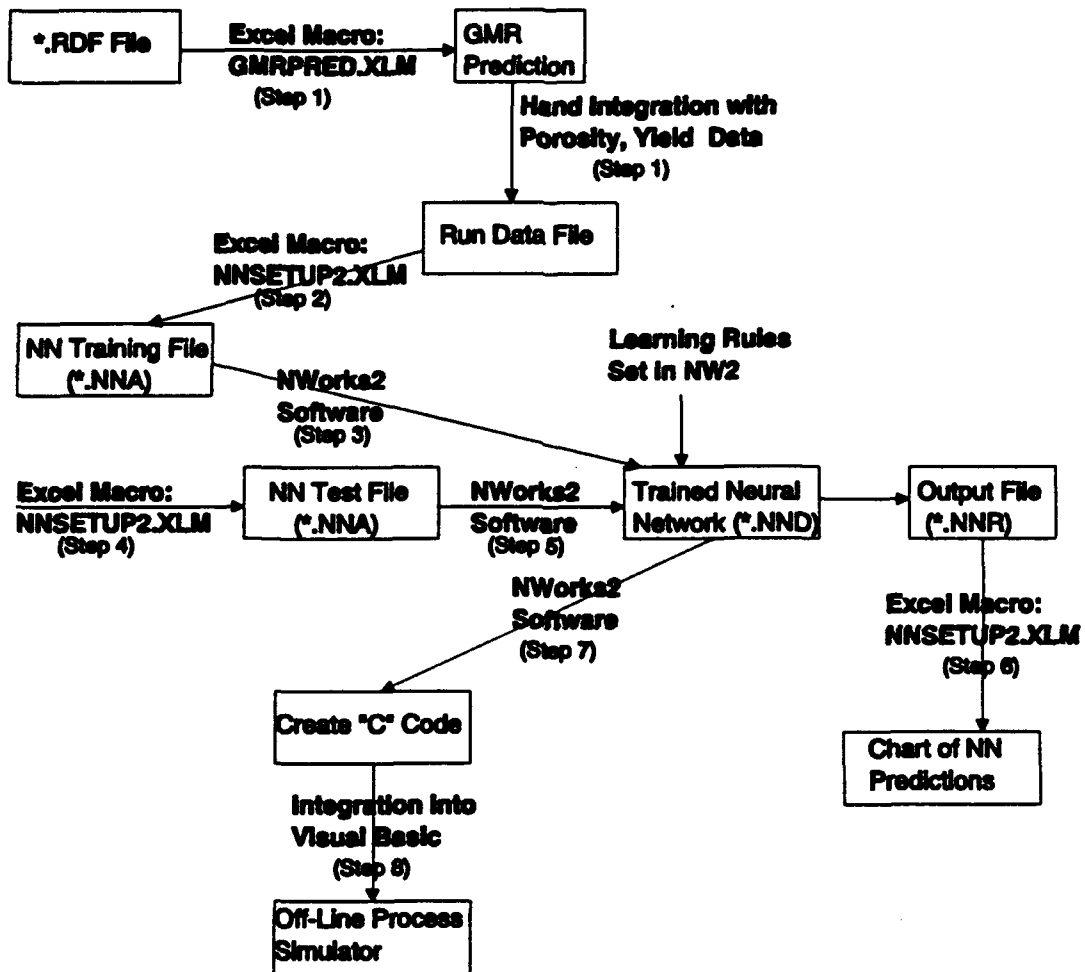
In NW2, neural networks that predict outputs as desired can be generated into "C" Code through the "Flash Code" Function.

### **Step 8**

In Visual Basic, the "C" Code generated by NW2 can be opened as text, transferred to the VB operating language and put together in a aesthetic visual display. The Visual Basic Program allows the user to input values and see the values that the neural network will predict for yield and porosity.

## FLOW CHART

The following chart shows the interrelationship between all the steps in creating neural networks.



## REFERENCES

1. Higginbotham, G. "Workshop on Fundamentals and Modeling," *Powder Metallurgy*, vol. 36, no. 4, 1993, pp. 248-249.
2. Payne, R.D., Moran, A.L., Madden, C.J. and Kelley, P., "An Optical Roughness Sensor for Real-Time Quality Measurement," *J. Metals*, vol. 43, no. 10, Oct. 1991, pp. 18-21.
3. Brooks, R.G., Leatham, A.G., Dunstan, G.R. and Moore, C., "Osprey Technology for Spray-Deposited Preforms and Powders in Superalloys," paper presented at Powder Metallurgy Superalloys conference, Nov. 18-20, 1980.
4. Moran, A.L., Palko, W.A., Madden, C.J., and Kelly, P. "Thick Section Alloy 625 Tubulars Produced via Spray Forming," 1990 Advances in Powder Metallurgy, vol. 1, Metal Powder Industries Federation, pp. 553-561.
5. Payne, R.D., Moran, A.L., Cammarata, R.C. "Relating Porosity and Mechanical Properties in Spray Formed Tubulars," *Scripta Met*, vol. 29, pp. 907-912.
6. Bylinsky, G. "Computers that Learn by Doing," *Fortune*, September 6, 1993, pp. 96-102.
7. Pollard, A. "What are Neural Networks?," *Sensor Review*, July 1990, pp. 115-116.
8. Freundlich, N.J. "Brain-Style Computers", *Popular Science*, February 1989, pp. 69-72, 110.
9. Wilson, A.C. and Wilson, D. "Neural Networks- Applications-Specific Problem Solvers," *ESD: The Electronic System Design Magazine*, February 1989, pp. 30-36.
10. Caudill, M. "Neural Network Training Tips and Techniques", *AI Expert*, January 1991, pp. 56-61.
11. Wilson, A. "Cranium Computing: Demystifying Neural Nets," *ESD: The Electronic System Design Magazine*, July 1988, pp. 38-41.
12. Payne, R.D., Matteson, M.A., Moran, A.L. "The Application of Neural Networks to Spray Forming Technology," *Int. J. Powder Metallurgy*, vol. 29, no. 4, October 1993, pp. 345-351.
13. Payne, R.D., Rebis, R.E., Moran, A.L. " Spray Forming Quality Predictions via Neural Networks," *J. Mat. Eng. and Perf.*, vol. 2, no. 5, pp. 693-702.

## DISTRIBUTION

		Center Distribution		
Copies		Copies	Code	Name
1	ONT 225	1	0113	Douglas
2	DTIC	1	0115	Caplan
		1	60	Wacker
		1	63	Singerman
		1	64	Fischer
		1	601	
		1	601	Ventriglio
		1	602	Morton
		1	603	Cavallaro
		1	61	Holsberg
		1	610s	
		1	612	Arora
		7	612	Payne
		3	612	Rebis
		1	614	
		1	615	
		1	342.1	TIC - C
		1	342.2	TIC - A
		2	3431	Office Services
		3	756	Madden

**REPORT DOCUMENTATION PAGE**Form Approved  
OMB No. 0704-0188

1. AGENCY USE ONLY (Leave blank)		2. REPORT DATE	3. REPORT TYPE AND DATES COVERED	
4. TITLE AND SUBTITLE <b>PROCESS CONTROL DEVELOPMENT FOR THE SPRAY FORMING PROCESS</b>			5. FUNDING NUMBERS <b>93-1-2812-753 94-1-6120-703</b>	
6. AUTHOR(S) <b>R.D. Payne</b>				
7. PERFORMING ORGANIZATION NAME(S) AND ADDRESS(ES) <b>Carderock Division Naval Surface Warfare Center Bethesda, MD 20084-5000</b>			8. PERFORMING ORGANIZATION REPORT NUMBER  <b>CRDKNSWC-TR-61-94-11</b>	
9. SPONSORING/MONITORING AGENCY NAME(S) AND ADDRESS(ES) <b>Mr. Ivan Caplan Code 0115 Annapolis, MD 21402-5067</b>			10. SPONSORING/MONITORING AGENCY REPORT NUMBER	
11. SUPPLEMENTARY NOTES				
12a. DISTRIBUTION/AVAILABILITY STATEMENT <b>Approved for public release; distribution is unlimited.</b>			12b. DISTRIBUTION CODE	
13. ABSTRACT (Maximum 200 words) <b>Spray forming is an alternate alloy production technique to both conventional and powder metallurgy methods. In an effort to develop process control of this process, relationships must be established between process parameters and product quality parameters. Because mathematical modeling of the spray forming process has not yet been able to determine well-defined relationships between process parameters and product quality, neural networks were employed to more clearly define this relationship. It was the goal of initial neural network development to prove the feasibility of neural network use in spray forming control. Because this initial work was successful, the focus of subsequent development was on determining and improving the accuracy of these neural network predictions. Not only can neural networks successfully predict trends in quality data, but they are as accurate as an experienced operator in predicting quality outputs. Finally, process control development resulted in a Windows compatible software program that puts neural network predictions within easy access for the spray forming plant operator.</b>				
14. SUBJECT TERMS <b>Spray Forming, Neural Networks, Process Control, Intelligent Processing</b>			15. NUMBER OF PAGES <b>21</b>	
			16. PRICE CODE	
17. SECURITY CLASSIFICATION OF REPORT <b>Unclassified</b>	18. SECURITY CLASSIFICATION OF THIS PAGE <b>Unclassified</b>	19. SECURITY CLASSIFICATION OF ABSTRACT <b>Unclassified</b>	20. LIMITATION OF ABSTRACT <b>Unclassified</b>	